Protolith and tectonic setting of an Archean quartzofeldspathic gneiss sequence in the Blacktail Mountains, Beaverhead County, Montana

by Michael Lee Clark

A thesis submitted in partial fulfillment of the requirements for the degree of Master of Science in Earth Sciences
Montana State University

Abstract:
High-grade quartzofeldspathic gneisses (QFGs) of Archean age are exposed in the Blackball Mountains of the northwestern Wyoming Province. Gneisses of dacitic to rhyolitic composition (69-76 weight percent SiO2) are the most common varieties of QFG and are interlayered with subordinate volumes of andesitic gneiss (56-59 weight percent SiO2). The QFGs are classified into mappable units based on mafic mineral content. Lesser volumes of mafic and ultramafic rocks are interlayered with the QFGs. Mafic rocks include primitive tholeiitic to calc-alkalic basalts and basaltic komatiites.

The protolith of these QFGs has been interpreted as supracrustal rocks by some workers and plutonic rocks by others. Characteristics of compositional layering; such as conformable lithologic contacts, intimate interlayering of gneiss types, interlayered marbles and calc-silicate gneisses; combined with the absence of igneous textures suggest that the quartzofeldspathic gneisses were derived from supracrustal rocks. However, geochemical discrimination indicates that most quartzofeldspathic gneisses were derived from igneous rocks. A protolith composed of volcanic and volcaniclastic rocks is compatible with both lines of evidence. Therefore, protolith of this Archean terrene is interpreted as a bimodal rhyolite/dacite-basalt series dominated by felsic rocks.

Trace element discrimination indicates that the parent magmas of the volcanics were generated in one of two environments: 1) an active continental margin adjacent to an intracratonic rift, or 2) a single environment with affinities to both. REE analyses suggest that the dacites were probably generated from partial melting of an eclogite, amphibolite, or garnet amphibolite source; and the rhyolites were probably generated from partial melting of older continental crust. Major-element characteristics, discriminant function analysis, and lithologic associations (compared to Phanerozoic rocks) suggest that the volcanic and volcaniclastic sediments were deposited in a continental rift basin.

The continental rift basin collapsed as a result of convergence and tectonic stacking of one basin-bounding, continental crust segment over the, other. Garnet-biotite and garnet-cpx geothermometry yield a temperature range of 740-810° C for peak metamorphism. Garnet-opx geobarometry and retrograde growth of cordierite from garnet+sillimanite+quartz indicate a minimum pressure of 5.1-6.2 kilobars for the peak metamorphism. Basin sediments were buried at least 20 kilometers and metamorphosed to granulite-grade conditions about 3.08 Ga ago.

PROTOLITH AND TECTONIC SETTING OF AN ARCHEAN QUARTZOFELDSPATHIC GNEISS SEQUENCE IN THE BLACKTAIL MOUNTAINS, BEAVERHEAD COUNTY, MONTANA

by

Michael Lee Clark

A thesis submitted in partial fulfillment
of the requirements for the degree

of

Master of Science

in

Earth Sciences

MONTANA STATE UNIVERSITY
Bozeman, Montana

May, 1987

APPROVAL

of a thesis submitted by

Michael Lee Clark

This thesis has been read by each member of the thesis committee and has been found to be satisfactory regarding content, English usage, format, citations, bibliographic style, and consistency, and is ready for submission to the College of Graduate Studies.

May 22, 1987
Date

David W. Mogk
Chairperson, Graduate Committee

Approved for the Major Department

22 May 1987
Date

Head, Major Department

Approved for the College of Graduate Studies

June 1, 1987
Date

Henry L. Parsons
Graduate Dean

STATEMENT OF PERMISSION TO USE

In presenting this thesis in partial fulfillment of the requirements for a master's degree at Montana State University, I agree that the Library shall make it available to borrowers under rules of the Library. Brief quotations from this thesis are allowable without special permission, provided that accurate acknowledgment of source is made.

Permission for extensive quotation from or reproduction of this thesis may be granted by my major professor, or in his absence, by the Director of Libraries when, in the opinion of either, the proposed use of the material is for scholarly purposes. Any copying or use of the material in this thesis for financial gain shall not be allowed without my written permission.

Signature Michael L. Clark

Date May 22, 1987

ACKNOWLEDGEMENTS

I thank my thesis advisor, Dr. David Mogk, for guiding this thesis project; for funding field work, thin sections, and geochemistry; and for providing access to the microprobe at the University of Washington. Many thanks to Dr. John Jutila, Vice President for Research at Montana State University, for funding field work for this thesis. I thank Dr. David Lageson for reviewing this manuscript and credit Dr. Lageson for encouraging me to participate in the graduate program at Montana State University. I am grateful to Dr. John Childs for intensively critiquing this manuscript, for visiting my study area, and for packing samples out of the Blacktail Mountains. I am obliged to Dr. Willard Keightly for being a part of my thesis committee and for engaging in stimulating conversation on topics ranging from evolution to orogeny. I also thank Dale Anderson for packing samples out of my study area and for his persistent and occasionally constructive badgering.

I am most grateful to my family, especially my mother, Marge Clark, whose enduring support has made this entire education possible. Thank you!

TABLE OF CONTENTS

TABLE OF CONTENTS--Continued

LIST OF TABLES

LIST OF FIGURES

LIST OF FIGURES--Continued

LIST OF FIGURES--Continued

LIST OF PLATES

ABSTRACT

High-grade quartzofeldspathic gneisses (QFGs) of Archean age are exposed in the Blacktail Mountains of the northwestern Wyoming Province. Gneisses of dacitic to rhyolitic composition (69-76 weight percent SiO_2) are the most common varieties of QFG and are interlayered with subordinate volumes of andesitic gneiss (56-59 weight percent SiO_2). The QFGs are classified into mappable units based on mafic mineral content. Lesser volumes of mafic and ultramafic rocks are interlayered with the QFGs. Mafic rocks include primitive tholeiitic to calc-alkalic basalts and basaltic komatiites.

The protolith of these QFGs has been interpreted as supracrustal rocks by some workers and plutonic rocks by others. Characteristics of compositional layering; such as conformable lithologic contacts, intimate interlayering of gneiss types, interlayered marbles and calc-silicate gneisses; combined with the absence of igneous textures suggest that the quartzofeldspathic gneisses were derived from supracrustal rocks. However, geochemical discrimination indicates that most quartzofeldspathic gneisses were derived from igneous rocks. A protolith composed of volcanic and volcaniclastic rocks is compatible with both lines of evidence. Therefore, protolith of this Archean terrane is interpreted as a bimodal rhyolite/dacite-basalt series dominated by felsic rocks.

Trace element discrimination indicates that the parent magmas of the volcanics were generated in one of two environments: 1) an active continental margin adjacent to an intracratonic rift, or 2) a single environment with affinities to both. REE analyses suggest that the dacites were probably generated from partial melting of an eclogite, amphibolite, or garnet amphibolite source; and the rhyolites were probably generated from partial melting of older continental crust. Major-element characteristics, discriminant function analysis, and lithologic associations (compared to Phanerozoic rocks) suggest that the volcanic and volcaniclastic sediments were deposited in a continental rift basin.

The continental rift basin collapsed as a result of convergence and tectonic stacking of one basin-bounding, continental crust segment over the other. Garnet-biotite and garnet-cpx geothermometry yield a temperature range of 740-810° C for peak metamorphism. Garnet-opx geobarometry and retrograde growth of cordierite from garnet+sillimanite+quartz indicate a minimum pressure of 5.1-6.2 kilobars for the peak metamorphism. Basin sediments were buried at least 20 kilometers and metamorphosed to granulite-grade conditions about 3.08 Ga ago.

CHAPTER 1

INTRODUCTION

Quartzofeldspathic gneisses comprise the bulk of late Archean crust that is preserved worldwide, yet their origins are much less well understood than the origins of volumetrically subordinate granite-greenstone belts (Condie, 1983; Windley, 1984; Taylor and McLennan, 1985). This study contributes to the understanding of quartzofeldspathic gneiss (QFG) terranes through examination of an Archean, high-grade, QFG terrane in the Blacktail Mountains of the northwestern Wyoming Province (see Figure 1).

Difficulties in determining the origins of QFG terranes throughout the world begin with the distinction between intrusive igneous and supracrustal (sedimentary and volcanic) protoliths (e.g., Perera, 1983). This study includes examination of a QFG sequence in the Blacktail Mountains which has been correlated with QFGs in the adjacent Ruby Range and has been interpreted as both orthogneiss (e.g., Heinrich and Rabbit, 1960) and paragneiss (Garihan and Okuma, 1974). Multiple high-grade tectonothermal events that are typically recorded in QFG terranes destroy primary textures that are diagnostic of plutonic or supracrustal protoliths (Condie, 1983; Windley, 1984; Nutman and others, 1984; Taylor and McLennan, 1985). Therefore, methods which do not rely solely on primary textures must be employed to establish the protolith of high-grade QFG terranes. Methods which

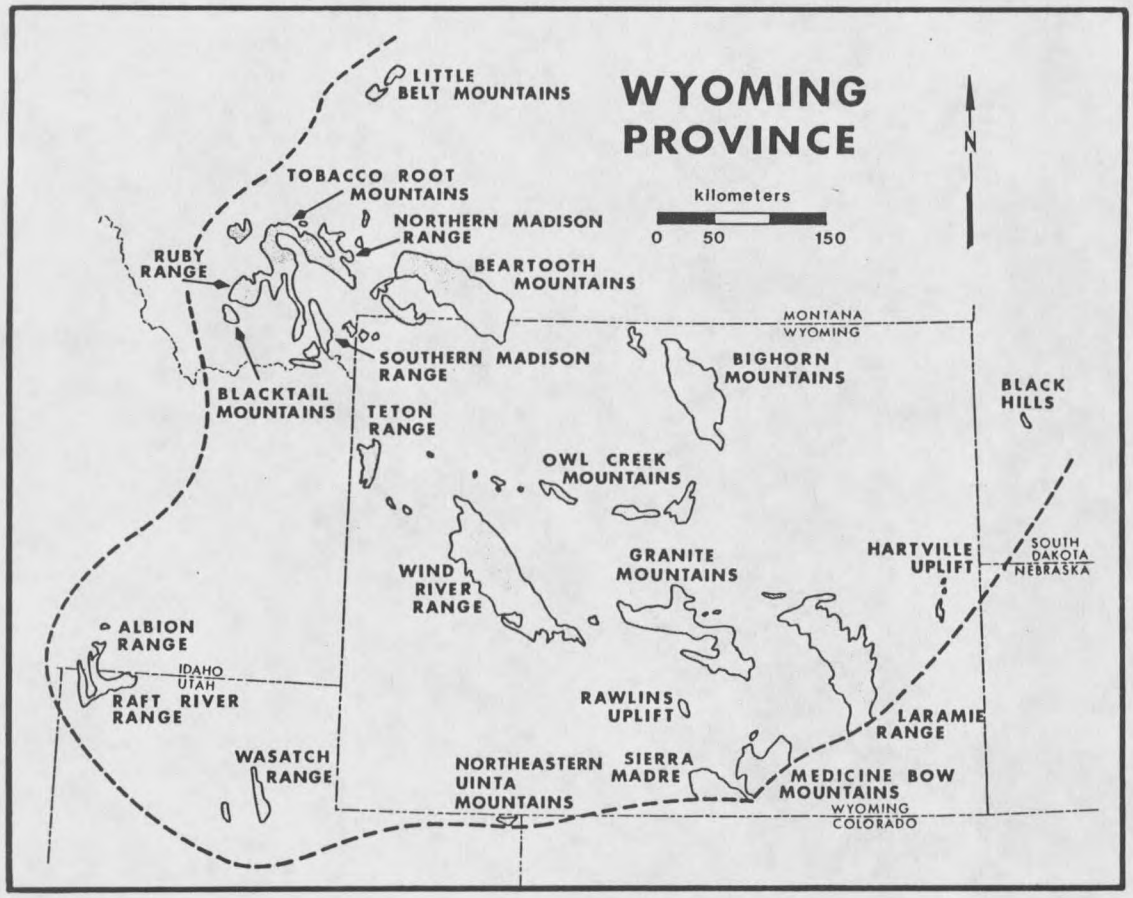

Figure 1. Distribution of Precambrian crystalline rocks is shown for the Wyoming Province (Condie, 1976; Karlstrom, 1979).

include examination of compositional zonation and general lithologic associations coupled with major and trace element geochemical discrimination are used in this study to arrive at reasonable deductions concerning the protolith of the QFGs in the Blacktail Mountains.

Distinction between orthogneiss (metamorphosed intrusive igneous rocks) and paragneiss (metamorphosed supracrustal rocks) is vital to

the interpretation of tectonic evolution of QFG terranes. For example, if a given suite of QFG is derived from supracrustal rather than plutonic rocks, episodes of sediment generation, sediment deposition, and basin development must be included in the history of the suite. Once the protolith is determined to be plutonic or supracrustal, additional characteristics can be evaluated to determine the tectonic environment in which the QFG terrane originated. The present study compares lithologic associations, whole rock geochemistry, and trace element geochemistry of Archean rocks in the Blacktail Mountains to Proterozoic and Phanerozoic rocks in order to establish the probable tectonic setting for the protoliths of QFGs exposed in the Blacktail Mountains.

CHAPTER 2

REGIONAL GEOLOGIC SETTING

Northwestern Wyoming Province

Figure 2 shows the distribution of Archean rocks of the northwestern portion of the Wyoming Province that are exposed within numerous Laramide (Schmidt and Garihan, 1983), basement-cored uplifts. The eastern Beartooth Mountains are composed of late Archean granitoids and volumetrically subordinate inclusions of older supracrustal rocks (Mueller and Wooden, 1982; Mueller and others, 1985). The North Snowy Block of the Beartooth Mountains contains tectonically juxtaposed meta-igneous and metasupracrustal rocks (Mogk, 1984: Mogk and Henry, 1987). The South Snowy Block consists of metasupracrustal rocks that were intruded by volumetrically subordinate late Archean granitoids (Casella and others, 1982; Thurston, 1986).

Uplifts west of the Beartooth Mountains are composed predominantly of complexly deformed Archean supracrustal sequences, of which quartzofeldspathic gneisses are the most common lithologies (e.g., Vitaliano and others, 1979; James and Hedge, 1980; Karasevich and others, 1981). Marble- and quartzite-bearing sequences were originally mapped as the "Cherry Creek Group" in the Gravelly Range (Peale, 1896). Sequences composed of quartzofeldspathic gneisses, schists and interlayered amphibolites, and which lack distinctive metasedimentary rocks (i.e., marbles and quartzites) were originally mapped as the

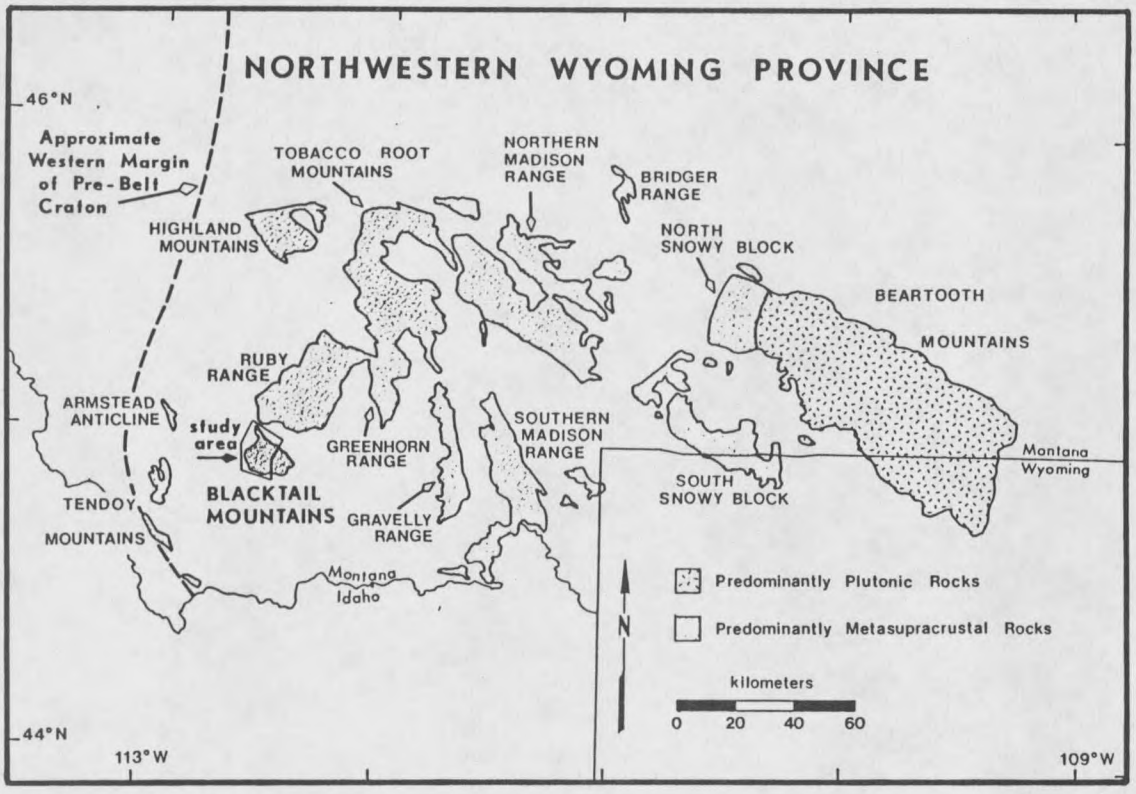

Figure 2. Distribution of Archean Rocks is shown for the northwestern Wyoming Province in southwestern Montana (Condie, 1976; Bergantino and Clark, 1985).

"Pony Series" in the Tobacco Root Mountains (Tansley and others, 1933). Although these designations have been widely applied to exposures west of the Beartooth Mountains, correlation between mountain ranges has been inconsistent (e.g., Reid, 1957; McThenia, 1960). More recently, the older nomenclature has been discarded in favor of lithologic descriptions (e.g., Hadley, 1969a, 1969b, 1980; Millholland, 1976; Vitaliano and others, 1979). Other studies have documented genetically distinct terranes between and within ranges

(Erslev, 1983; Thurston, 1986; Salt, 1987; Mogk and Henry, 1987). However, the depositional environment and pre-metamorphic history of these Archean supracrustal rocks are still poorly understood.

Compositional layering within most ranges strikes generally NE-SW and dips variably (Hadley, 1969b; Spencer and Kozak, 1975; Tilford, 1978; Berg, 1979; Vitaliano and others, 1979; Karasevich, and others, 1981; Erslev, 1983). However, compositional layering is broadly warped into E-W and NW-SE trends in the Highland Mountains, the northern Tobacco Root Mountains and the northern Ruby Range (Duncan, 1976; Vitaliano and others, 1979; Karasevich, 1980, 1981). Compositional layering has been affected by at least two generally recognized folding events: earlier isoclinal folding and later coaxial, tight-to-open (infrequently isoclinal) folding (Spencer and Kozak, 1975; Garihan, 1979; Vitaliano and others, 1979; Wilson, 1981; Erslev, 1983). However, the number of folding events and the structural style reported for different areas are variable and may reflect a unique tectonic history for each range and for various structural units within a single range.

Two dominant metamorphic events are recognized throughout the Archean sequences west of the Beartooth Mountains. The first event, M1, produced assemblages characteristic of upper amphibolite grade to granulite grade with temperature and pressure conditions of 600-750^{o} C and 4-8 kilobars (Wier, 1965; Dahl, 1979a; Immega and Klein, 1976; Desmarais, 1981; Karasevich and others, 1981; Kleinschmidt, 1981; and Erslev, 1983). A pre-M1, granulite-grade metamorphic event has been suggested for a location in the Tobacco Root Mountains (Mueller and

Cordua, 1976). The second event, M2, produced assemblages characteristic of greenschist grade to almandine-amphibolite grade which overprinted earlier upper amphibolite-grade to granulite-grade assemblages (Wier, 1965; Giletti, 1966; Dahl, 1979a; Kleinschmidt, 1981; and Erslev, 1983). K-Ar and Rb-Sr analyses reported to date indicate an age of 2.6-2.8 Ga for M1 (Giletti, 1966, 1971; Mueller and Cordua, 1976; James and Hedge, 1980). A mineral age on micas of 1.4-1.7 Ga has been interpreted as the age of M2 (Giletti, 1966, 1971; James and Hedge, 1980). There is some indication of older rocks. Rb-Sr whole rock ages of 3.25 Ga have been reported for a quartzofeldspathic gneiss in the eastern portion of the northern Madison Range and 3.08 Ga for a quartzofeldspathic gneiss in the Blacktail Mountains (Giletti, 1966, 1971; James and Hedge, 1980).

Blacktail Mountains

The Archean sequence in the Blacktail Mountains includes dominant volumes of quartzofeldspathic gneiss; subordinate volumes of amphibolite, garnet-biotite gneiss, and ultramafite; and local occurrences of calc-silicate gneiss, marble and quartzite. Compositional layering strikes generally NE-SW and has been affected by at least two periods of folding: tight-to-isoclinal folding followed by coaxial open folding. Granulite-grade assemblages have been preserved in certain mafic rocks and felsic gneisses. Giletti (1966) reported a Rb-Sr whole-rock model age for one horizon in the QFG of 3.08 Ga, assuming initial $^{87}Sr/^{86}Sr = 0.710$.

Most of the Archean rocks west of the Beartooth Mountains are believed to have had supracrustal origins. However, the protolith of a unit of QFG that has been correlated between the Blacktail Mountains and the Ruby Range (the "Dillon Granite Gneiss," Scholten and others, 1955; Heinrich, 1960) is still disputed. The "Dillon Granite Gneiss" has been interpreted as an orthogneiss (Garihan and Okuma, 1974) and as a paragneiss (Garihan and Williams, 1976). The Blacktail Mountains host the original type locality of this disputed unit (Heinrich, 1948, 1950, 1953; Scholten and others, 1955). Evidence regarding the nature of the protolith for the "Dillon Granite Gneiss" is discussed later in this report.

CHAPTER 3

LITHOLOGIES

Felsic Gneisses

Quartzofeldspathic gneisses (QFGs) are the volumetrically dominant lithologies of the Archean sequence in the Blacktail Mountains (see Plate I). QFGs are composed of quartz and variable amounts of potassium and plagioclase feldspars and are distinguished by their dominant mafic phases. Varieties include biotite-hornblende+/-diopside QFG (BH), garnet-biotite-hornblende QFG (GBH) and pyroxene-magnetite-hornblende QFG (PMH). BH, GBH, and PMH are compositionally layered on a centimeter-to-meter scale. Compositional layering is characterized by variations in both potassium feldspar/plagioclase ratios and mafic/felsic phase ratios (see Figure 3). A fourth QFG of granitic (senso stricto) composition (G) is composed of biotite-hornblende-quartz-plagioclase-microcline. Microcline in G is characteristically dull-pink to dull-red. G is compositionally layered on a centimeter scale but is homogeneous on a greater-than-decimeter scale. Although compositionally variable, the felsic gneisses exhibit similar macroscopic and microscopic fabric elements.

Table 1 summarizes modal compositions of the felsic gneisses. The quartz/potassium feldspar/plagioclase ratios of the felsic gneisses are plotted on an igneous rock classification diagram in Figure 4 (Streckheisen, 1976, 1979). Varieties of BH and GBH units plot in

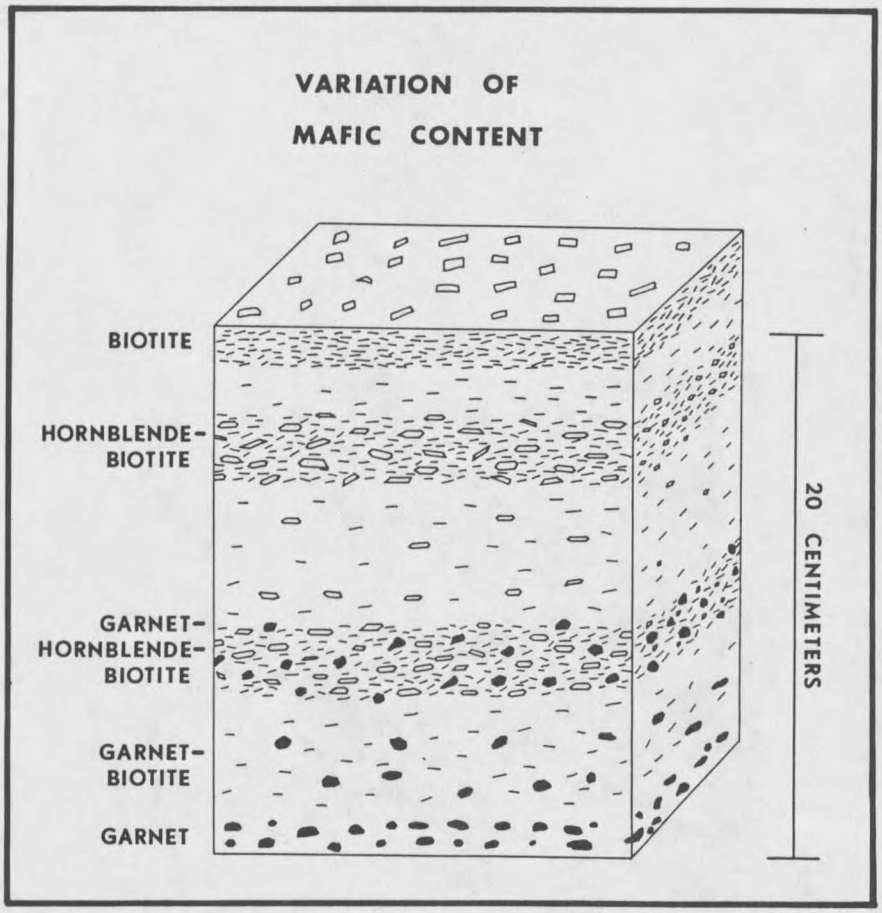

Figure 3. The distribution of mafic phases, which characterize compositional layering, is shown in a schematic block diagram.

the rhyolite and dacite fields. PMH and G plot in the rhyolite field. Plagioclase composition in BH varies between layers from oligoclase (An_{10}) to andesine (An_{40}). Potassium feldspar in the felsic gneisses is typically microcline. However, orthoclase is present in some samples of BH and GBH, and is dominant over microcline in PMH. Gradation from untwinned orthoclase to cross-hatch twinned microcline is present in some BH and GBH samples. The potassium feldspar in G is exclusively microcline.

Table 1. Modal Mineralogy of Felsic Gneisses

	BH	GBH	PMH	G
N	15	10	1	1
QUARTZ	17-52%	2-70%	27%	26%
PLAGIOCLASE	18-65	7-55	35	23
K-FELDSPAR	3-49	0-40	27	42
BIOTITE	tr-7	tr-24	0	2
GARNET	0	tr-15	0	0
SILLIMANITE	0	0-10	0	0
CORDIERITE	0	0-10	0	0
HORNBLENDE	tr-8	0	5	7
DIOPSIDE	0-11	0	2	0
HYPERSTHENE	0	0	2	0
OPAQUES	tr-4	tr-1	2 (magnetite)	tr
APATITE	tr-2	tr	tr	tr
ZIRCON	tr-1	tr	tr	tr
HERCYNITE	0	tr	o	0

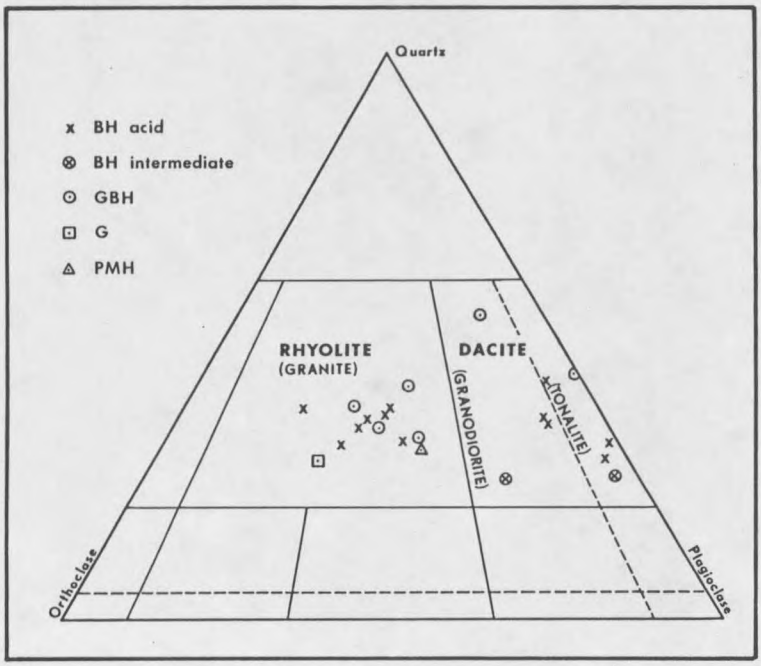

Figure 4. Samples of the felsic gneisses are plotted on a Streckheisen igneous rock diagram (Streckheisen, 1976, 1979). Samples are rhyolitic to dacitic in composition.

Figure 5 illustrates the variability of major phases within the BH and GBH units. The BH unit consists of two varieties, distinguished by the total percentage of all mafic minerals present (i.e., color index): BH-ACID (color index = 0-20) and BH-INT (color index = 20-40). In BH-ACID layers, hornblende and biotite coexist in one variety and are mutually exclusive in other varieties. BH-INT layers are characterized by hornblende+/-biotite+/-diopside. BH-INT layers account for only a minor volume of the BH units. The GBH unit is composed of garnet+biotite layers locally intercalated with hornblende+/-biotite+/-garnet layers. In some GBH horizons, garnet is the only mafic phase present. Sillimanite is present, with garnet and biotite, as disseminated grains and as fine-grained mats in some GBH samples. Apatite, opaque phases, and subhedral to well-rounded zircon grains are common accessory phases in all felsic gneisses. Accessory opaques, zircon and apatite are locally concentrated in mafic-rich laminae. The G and PMH units are compositionally layered on a millimeter-to-centimeter scale, but are homogeneous on an outcrop scale. G and PMH are locally interlayered with BH and GBH horizons. All felsic gneiss units are mutually conformable.

Many fabric elements are common to all felsic gneisses. Compositional layering is conformable and gradational at all scales (see Figure 3). Mafic phases are concentrated in discrete laminae as well as disseminated throughout horizons between mafic-rich laminae. Disseminated biotite grains are typically parallel to compositional layering, but are locally discordant. In cases where disseminated biotite grains are discordant to compositional layering, the biotite

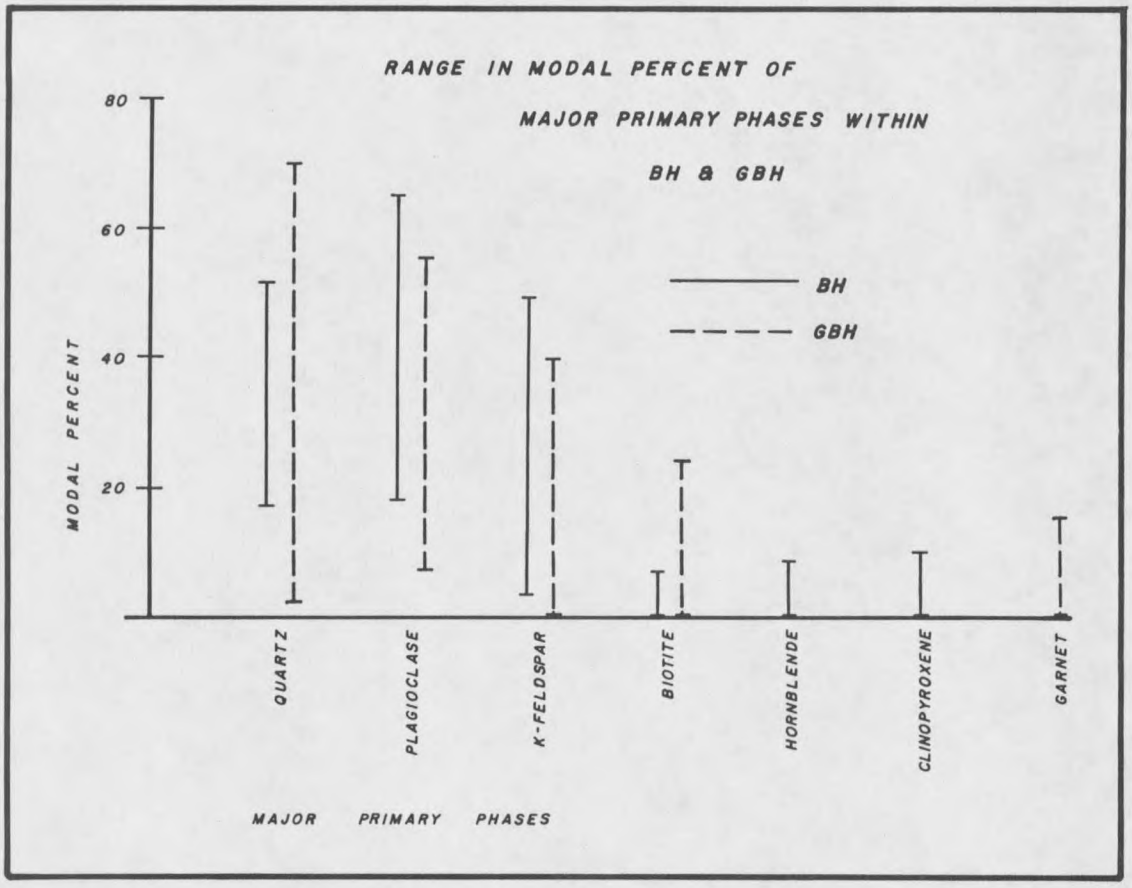

Figure 5. Range in modal percent of major primary phases is shown for gneisses of the BH and GBH units.

grains within mafic laminae are aligned parallel to the disseminated biotite grains. Quartz ribbons and tabular groups of feldspar grains define a felsic-grain foliation that is most prominent in gneisses with low color index (CI < 6). Subgranoblastic and granoblastic textures are locally developed in all felsic gneisses. Quartz ribbons are thoroughly recrystallized and exhibit strain-free subdomains in samples with a granoblastic feldspar population. In samples of GBH, garnets occur concentrated in laminae as well as disseminated in

horizons between garnet-rich laminae. Larger garnets within garnet-rich laminae are elongated (length/width = 5) and form ameboid poikiloblasts with inclusions of all other primary phases. Smaller garnets are free of inclusions and are usually hypidioblastic.

All felsic gneisses are locally migmatitic. The migmatite horizons are similar to stromatic migmatites described by Johannes and Gupta (1982). Thin, coarse-grained lenses within a medium-grained host characterize migmatitic textures in the Blacktail Mountains. The coarse-grained lenses are commonly 1-5 centimeters thick and 10-30 centimeters in both length and width. The coarse-grained lenses are parallel or subparallel to compositional layering. These lenses occur both isolated and connected by veinlets which cut across compositional layering for short distances (tens of centimeters). Coarse-grained lenses are weakly foliated to nonfoliated, and truncate compositional layering. Minerals present in the host QFG are also present in the coarse-grained layers, though not necessarily in the same proportions. Mafic grains in these coarse-grained lenses are often concentrated into selvages at lens margins. These migmatite textures are interpreted to result from <u>in situ</u> melting and recrystallization associated with a high-grade metamorphic event (Johannes and Gupta, 1982).

In isolated cases, the coarse-grained lenses of the migmatite horizons can be traced from millimeter-thick, medium-grained leaves into coarse-grained veins several centimeters thick. Locally, these lenses extend into zones where several lenses coalesce to form thick (5-30 centimeters), irregularly shaped bodies. In such cases, layers of the medium-grained, host felsic gneiss can be traced into ptygmatic

folds within the coarse-grained body. Localized ptygmatic folding associated with stromatic migmatites suggests that migmatite formation and the high-grade metamorphic event were coeval with an episode of folding.

Mafic and Ultramafic Rocks

Mafic rocks are subordinate in volume to felsic gneisses (see Plate I), and are highly variable in texture and composition. Mafic rocks include foliated amphibolite layers, foliated granulite layers, weakly foliated to unfoliated ultramafite lenses, and unfoliated gabbroic dikes. The amphibolite layers are conformable to the host felsic gneisses. Contacts between amphibolite layers and felsic gneisses vary from abrupt to gradational. The granulite layers exhibit sharp contacts with the BH felsic gneisses. A 1-2 centimeters-thick biotite selvage is present at the contacts of the granulite layers. Unfoliated ultramafite lenses are commonly oriented with their long axes parallel to compositional layering in the host felsic gneisses. The unfoliated gabbroic dikes trend west to northwest and cross-cut foliation in the felsic gneisses. Table 2 summarizes modal mineralogy of the mafic and ultramafic rocks.

Amphibolites occur as 10 centimeters- to 5 meters-thick layers intercalated within felsic gneisses, and as larger map-scale bodies (i.e., units extensive enough to be distinguished on Plate I). Amphibolite layers which are tens-of-meters thick and interlayered with felsic gneiss layers of similar thickness and are designated as IG (interlayered gneisses) on Plate I. Amphibolite layers are continuous

across their outcrops. Some layers maintain uniform thickness along their exposures, while others pinch and swell. Some map-scale amphibolite layers form lens-shaped bodies. Exposures of other map-scale amphibolite bodies are limited, and their lens shape is inferred. At one location, a 0.5-2 meter-thick, biotite-rich selvage separates the largest map-scale amphibolite body from the host BH gneiss. Amphibolite layers exhibit centimeter-scale compositional layering, but are compositionally homogeneous on a greater-than-decimeter scale. This layering is parallel to compositional layering in the host felsic gneiss. The amphibolites are composed predominantly of quartz-plagioclase-hornblende+/-biotite+/-clinopyroxene. Quartz-feldspar lenses, devoid of mafic minerals, are present in some amphibolite layers. The quartz-feldspar lenses are 2 millimeters to 3 centimeters thick and occasionally form isoclinal and sigmoidal folds which have detached fold hinges. Hornblende-rich zones form thin (1-10 millimeters) halos around quartz-plagioclase lenses. The presence of hornblende-rich halos implies that the quartz-feldspar lenses were formed by either metamorphic differentiation or *in situ* melting. Hornblende grains are oriented parallel to compositional layering. A hornblende lineation is found on compositional layering surfaces in the amphibolites.

A few map-scale amphibolite bodies include garnetiferous layers. The garnets form poikiloblasts and are both disseminated and concentrated in garnet-rich laminae. Hornblende inclusions within garnet poikiloblasts are parallel to compositional layering. Snowball textures, characteristic of grain rotation during growth, are not

present in these garnets. The lack of snowball textures and the parallel geometry of the included grains indicate that these garnets grew after the completion of deformation which warped the quartz-feldspar lenses into isoclinal and sigmoidal folds.

Granulite bodies were found in two locations in the study area. Both exposures are in the northwestern canyon walls along Jake Creek, in the northern portion of the map area. The bodies are conformable to compositional layering in the host BH. Faint millimeter-scale, discontinuous, compositional layering within the granulite layers is parallel to compositional layering in the host felsic gneiss. The granulite bodies are composed predominantly of plagioclase-cummingtonite-hypersthene. At the northern of the two exposures, the contact between the granulite layer and the felsic gneiss is curved and

Table 2. Modal Mineralogy of Mafic and Ultramafic Rocks

	AMPHIBOLITES	GRANULITE BODY	ULTRAMAFITE	GABBROIC DIKE
N	5	1	1	1
QUARTZ	2-5%	0%	0%	2%
PLAGIOCLASE	31-56	9	0	36
BIOTITE	0-15	tr	0	9
AMPHIBOLE	24-50 HBD*	44 CUMM**	68 HBD*	6
CLINOPRYOXENE	0-15	0	0	24
HYPERSTHENE	0	47	30	23
OPAQUES	0-1	tr	2	tr
APATITE	tr	tr	0	0
ZIRCON	tr	tr	0	0

*HBD = Hornblende
**CUMM = Cummingtonite

parallel to curved compositional layering in the felsic gneiss. In this outcrop, both the granulite layer and the felsic gneiss have been folded.

Ultramafites form thin, weakly foliated to nonfoliated lenses that are generally elongated parallel to compositional layering in the felsic gneisses. In some cases, the ultramafites are slightly discordant to compositional layering in the felsic gneiss. The ultramafites are composed predominantly of hypersthene-hornblende. Three map-scale ultramafites, located in the northern portion of the map area, are nearly in alignment and are parallel to compositional layering in the felsic gneiss host. These aligned bodies may be remnants of a single disrupted layer.

West- to northwest-trending, nonfoliated, gabbroic dikes cut compositional layering in the felsic gneisses at high angles. At a location where the units are well exposed, a dike cuts across an amphibolite-BH contact. The dike does not have chilled margins and its contact is abrupt. Thin section analysis reveals a porphyritic texture characterized by hypersthene phenocrysts and quartz, diopside and plagioclase grains in the groundmass. Amphibole and biotite are present as grains that are smaller than typical groundmass grains and represent later growth.

Marble and Calc-silicate Gneiss

Marble and calc-silicate gneiss layers occur within the GBH unit in the southeastern corner of the study area. Although GBH is the dominant map unit in this area, GBH is interlayered with thin

conformable layers of BH and G. The calc-silicate gneisses are composed primarily of diopside-potassium feldspar-plagioclase-quartz. The marbles are composed primarily of calcite-dolomite-diopside-scapolite+/-graphite. Marble and calc-silicate gneiss occur interlayered within the GBH unit. Some horizons of marble and calc-silicate gneiss include thin layers of amphibolite.

CHAPTER 4

CONDITIONS OF METAMORPHISM

Peak Metamorphism

High-temperature and high-pressure conditions of the peak metamorphic event have formed granulite-grade assemblages throughout the sequence in rocks of appropriate composition. The assemblage hypersthene-cummingtonite-plagioclase is present in the mafic granulite bodies. The assemblage hypersthene-diopside-hornblende in the PMH unit is characteristic of granulite grade in felsic rocks. Diopside is typically present in the BH-INT gneisses. Plagioclase grains are locally antiperthitic, and potassium feldspar grains are locally orthoclase, indicating high-temperature crystallization. Granoblastic textures are locally well developed in all gneisses. In BH and GBH gneisses, biotite grains are characteristically red to red-brown and are indicative of granulite-grade metamorphism (Schreurs, 1985). The presence of locally well-developed, stromatic migmatites in all felsic gneisses indicates that in situ melting was associated with the high-temperature, peak metamorphism (Johannes and Gupta, 1982).

Microprobe analyses reveal that biotite grains from one GBH sample are unusually rich in titanium, containing 4.1 to 5.6 weight percent TiO_2 (weight percent is abbreviated "wt.%" hereafter). High-titanium content is an indication of high metamorphic grade (Kwak, 1968; Guidotti, Cheney and Guggenheim, 1977; Dymek, 1983). Schreurs (1985)

found that biotite grains with more than 0.45 atoms of Ti per 22 oxygen atoms were associated with low-to-intermediate, granulite-grade conditions and crystallization temperatures of greater than 750°C. Biotite grains in the sample from the Blacktail Mountains contain 0.47-0.65 atoms of Ti per 22 oxygen atoms, and are thus another indication of granulite-grade metamorphism.

Compositional data were collected with a microprobe at the University of Washington, in Seattle, for garnet and biotite grains in one sample and for diopside and garnet grains in another sample. Garnet-biotite geothermometry yields a temperature range of 740-810°C, with an assumed pressure of 7 kilobars (Ganguly and Saxena, 1984, 1985; Indares and Martignole, 1985). Cpx-garnet geothermometry yields a temperature of 750°C (Ellis and Green, 1979). Both geothermometers produce similar temperature estimates. Although the microprobe sample population is small, a temperature range of 740-810°C is inferred for peak metamorphism.

The garnet-biotite sample, used above in temperature modeling, contains the assemblage garnet-biotite-sillimanite-cordierite-microcline-plagioclase-quartz. Cordierite forms rims around garnet grains and represents retrograde mineral growth. A pressure estimate may be obtained from the reaction

$$3\text{Cordierite} = 2\text{garnet} + 2\text{sillimanite} + 5\text{quartz}.$$

Thompson (1976) has derived a geobarometer in which isopleths of magnesium content in cordierite and magnesium contents in garnet are plotted on a P-T-X diagram. Magnesium content in cordierite and garnet

increases with increasing pressure. Application of Thompson's (1976) model to the sample from the Blacktail Mountains yields a pressure estimate of 5.1-6.2 kilobars, in which mole fraction Mg^{++} in garnet is equal to 0.21-0.29 (from microprobe data) and the temperature of metamorphism is assumed to be 740°-810° C (see Figure 6). An additional pressure estimate is available using garnet-orthopyroxene

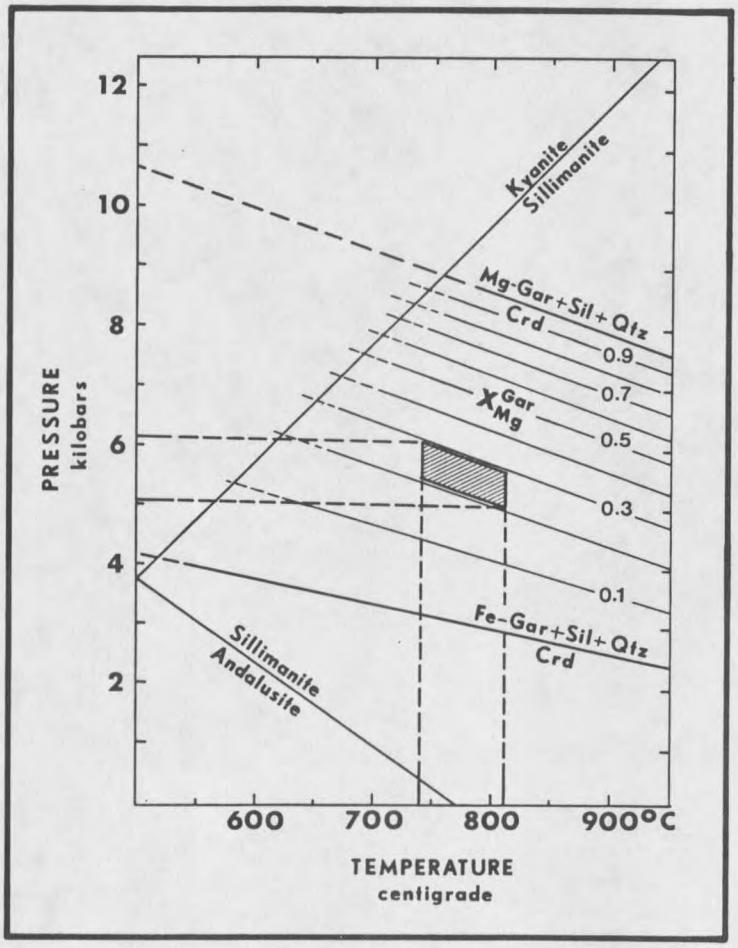

Figure 6. The P-T-X diagram of Thompson (1976) yields a pressure estimate of 5.1-6.2 kilobars for peak metamorphism. Mol fraction Mg^{++} in garnet, which varies from 2.1 to 2.9, and temperature estimates for peak metamorphism, which vary from 740° C to 810° C, constrain the pressure estimate (shaded area).

geobarometry. Garnet-orthopyroxene microprobe data were obtained from another sample containing coexisting garnet-orthopyroxene-plagioclase-quartz. The garnet-orthopyroxene geobarometry model of Newton and Perkins (1982) yields a pressure estimate of 5.6-6.2 kilobars. Pressure estimates from these two models are similar and indicate a pressure range of 5.1-6.2 kilobars for the peak metamorphism. However, Dahl (1979b) associated coexisting garnet and cordierite with retrograde metamorphism in similar rocks in the Ruby Range. Cordierite in the sample from the Blacktail Mountains is also retrograde, and thus 5.1-6.2 kilobars should be considered a minimum pressure for peak metamorphism of the sequence in the Blacktail Mountains.

Lower Temperature Re-equilibration

Temperature modeling of garnet rims and biotite grains tangential to garnet grains, as well as microscopic textures attest to pressure and temperature conditions of mineral equilibrium lower than conditions of the peak metamorphic event. Application of the garnet-biotite geothermometry models of Ganguly and Saxena (1984) and Indares and Martignole (1985) to microprobe data from garnet rims and tangent biotites yields temperatures of 500-550^{o}C. Petrography reveals several textures characteristic of re-equilibration. Albite rims are developed around plagioclase grains in many samples. Myrmekite is locally well developed within plagioclase grains. In some samples, potassium feldspar varies from untwinned grains to grains with well-developed cross-hatch twinning. These lower temperature conditions may be a result of either a cooling period after the peak metamorphism or a

regional retrograde metamorphic event. Garihan (1979) noted similar textures from gneisses in the Ruby Range and ascribed them to a cooling period after peak metamorphism. The similarity of textures described by Garihan (1979) to textures seen in the present study suggests that rock sequence in the Blacktail Mountains may have been subject to a cooling period after peak metamorphism comparable to that inferred for terranes in the Ruby Range. Garnet-biotite geothermometry suggests that the sequence cooled to 500-550^{o}C during the final stages of metamorphic recrystallization.

CHAPTER 5

PENETRATIVE STRUCTURE

Compositional layering is typically planar to gently undulating. However, this fabric is locally strongly sinuous and warped into isoclinal folds, some of which exhibit extremely attenuated and detached limbs. Planar rock fabric is typically accompanied and locally replaced by mineral lineations. Mineral lineations are defined by individual hornblende grains, quartz rods, linear aggregates of biotite grains, and linear aggregates of feldspar grains (Hobbs and others, 1976). Mineral lineations are developed in the plane of compositional layering and are best developed in the hinge regions of isoclinal folds. The lineations parallel the fold axes, and appear to have formed during isoclinal folding.

Planar and linear fabric data and field observations indicate two generations of coaxial, tight-to-isoclinal folds (F1 and F2). The isoclinal folds were subsequently refolded into open folds (F3, see Figure 7(b)). F1 is recorded only in rare cases as isoclinally refolded isoclinal folds. Tight-to-isoclinal folds that have not been isoclinally refolded are designated as F2. F2 is the dominant tight-to-isoclinal folding event (see Plate II). F2 transposed compositional layering and produced northeast- to southwest-trending, southwest-plunging, large scale (wavelength = tens of meters) and small scale (wavelength less than 1 meter) isoclinal folds with subvertical axial

surfaces. F2 axial surfaces are parallel to compositional layering (see Figure 7(a)). F2 also produced the mineral lineations that are parallel to F2 fold axes.

Biotite grains were rotated parallel to the axial surfaces of F3 open folds and form an axial planar foliation. The biotite grains retained their red-brown color through this event. Schreurs (1985) believes that "the clearest compositional change of biotite is expressed by their color variation: green-greenish brown in medium-grade rocks and reddish brown in granulite-facies rocks." The red-brown color of the re-oriented biotite grains suggests, therefore, that

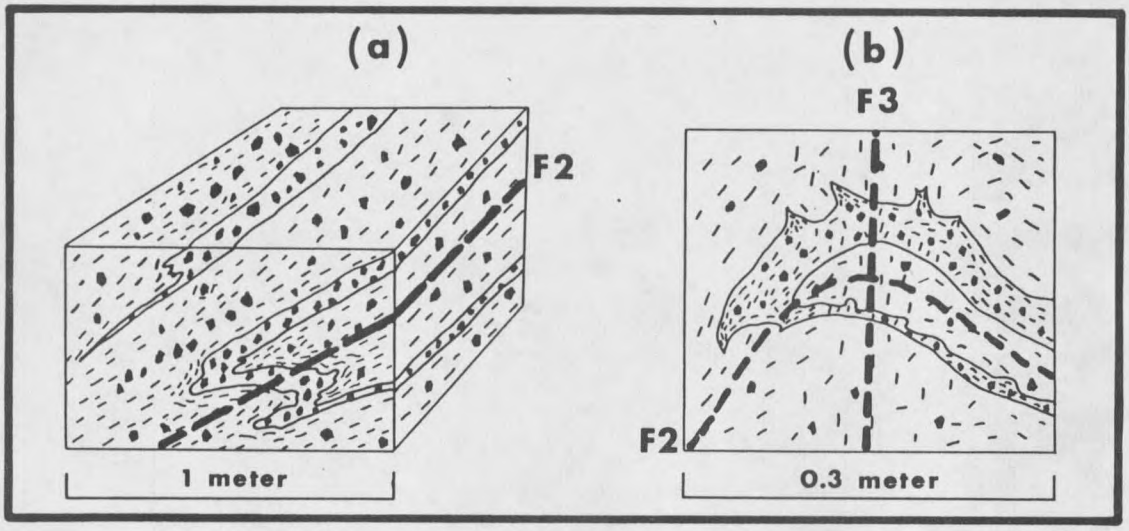

Figure 7. <u>(a) left</u> - A field sketch shows the axial surface of an isoclinal fold (F2) that is parallel to compositional layering. <u>(b) right</u> - A field sketch shows an isoclinal fold (F2) that has been refolded into an open fold (F3). Red-brown biotite grains are re-oriented parallel to the axial surface of F3.

the biotite recrystallization and the attendant folding event probably occurred under granulite-grade conditions. This conclusion is based solely on color of the recrystallized biotite grains and should be considered preliminary. Microprobe data should be collected and temperature modeling performed in order to test this hypothesis. F3 folding may be an effect of progressive deformation associated with the granulite-grade event that produced isoclinal folds, or it may be a separate folding event. However, multiple, granulite-grade deformational events have not been recognized in the Blacktail Mountains or in similar terranes in the Ruby Range (e.g., Garihan, 1979; Karasevich and others, 1981). Consequently, the F3 open-folding event which has affected the Archean sequence in the Blacktail Mountains is interpreted as an effect of progressive deformation subsequent to earlier isoclinal folding.

Figure 8 is a lower hemisphere, equal-area, stereographic projection of poles to compositional layering in the felsic gneisses. Although the projection does not uniquely define multiple fold generations, it does allow the interpretation suggested by field evidence (i.e., isoclinal folds have been refolded by open folding). The great circle drawn in Figure 8 depicts folds with generally steeply dipping limbs and sub-vertical axial surfaces, which strike northeast to southwest. The corresponding beta-pole depicts folds which plunge to the southwest (31^{o}, 229^{o}). However, the data pattern allows the great circle and corresponding beta-pole to be drawn with considerable variation. The geometry of folds suggested in Figure 8 is consistent

with field observations, which indicate that attitudes of tight-to-isoclinal and open folds are variable but plunge and trend generally southwest over most of the study area. However, mineral lineation data (discussed below) indicate that tight-to-isoclinal folds plunge northeast in the northernmost portion of the map area (see Plate I).

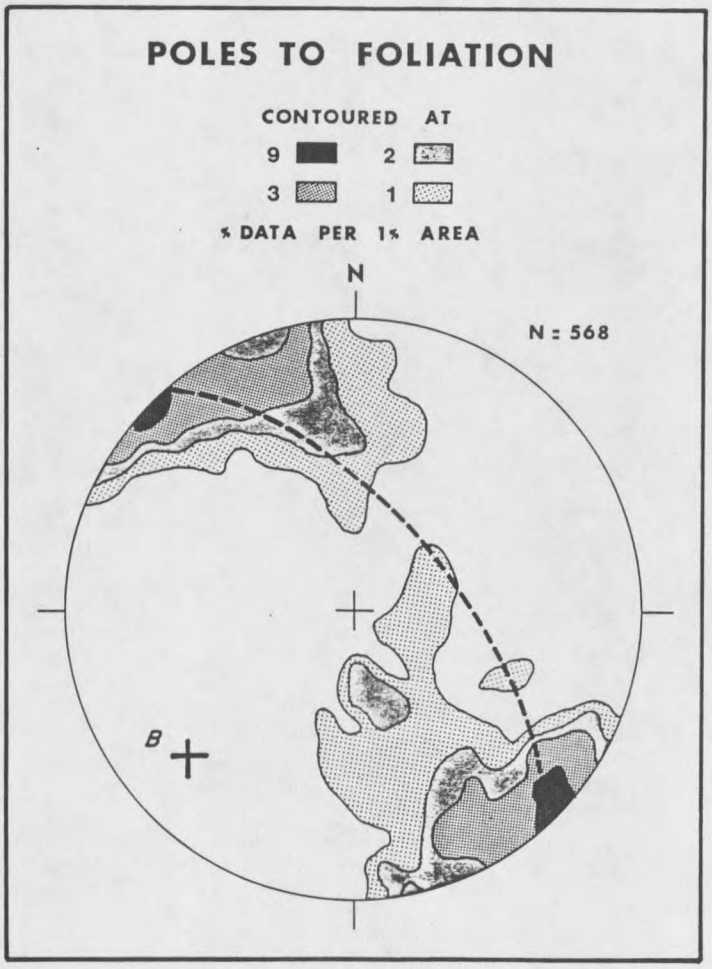

Figure 8. Poles to compositional layering within felsic gneisses are plotted on a lower hemisphere, equal-area, stereographic projection. Folds, depicted by the great circle, trend northeast to southwest. The position of the beta-pole (26^{o}, 229^{o}) indicates that folds plunge generally southwest over most of the map area.

Figure 9 is a lower hemisphere, equal-area, stereographic projection of attitudes of mineral lineations. Field evidence suggests that mineral lineations were formed parallel to F2 fold axes during tight-to-isoclinal folding. Position of the highest density area (solid black) indicates that the folds plunge and trend to the

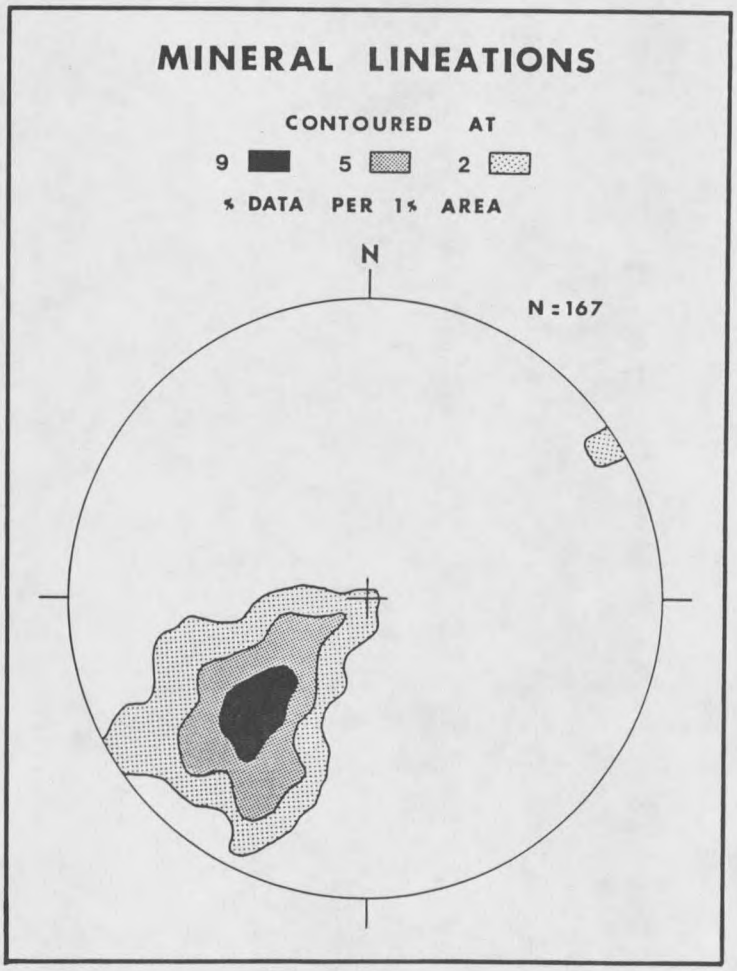

Figure 9. Attitudes of mineral lineations within the felsic gneisses are plotted on a lower hemisphere, equal-area, stereographic projection. Position of the highest density area (solid black) indicates that most lineations plunge and trend generally southwest (32^{o}-62^{o}, 214^{o}-237^{o}) over most of the study area.

southwest (32^{o}-62^{o}, 214^{o}-237^{o}) over most of the study area. However, mineral lineations in the northernmost portion of the map area plunge northeast and indicate that F2 folds plunge northeast in this vicinity (see Plate I). The pattern of the stereographic projection in Figure 9 is consistent with an interpretation of lineations which are coaxial to F2 and were dispersed by F3 folding. The lineation pattern is compatible with the variable southwest plunge of folds indicated by Figure 8.

CHAPTER 6

GEOCHEMISTRY

Felsic Gneisses

Major-element oxide, trace-element and normative mineralogy data for the felsic gneisses are presented in Table 3. BH is comprised of acidic gneisses (69-76 wt.% SiO_2, BH-ACID) interlayered with subordinate volumes of intermediate gneisses (56-59 wt.% SiO_2, BH-INT). GBH, PMH and G are comprised of acidic gneisses. BH-ACID, BH-INT, GBH, G, and PMH are plotted on Harker diagrams in Figure 10. Although sampling is limited, the Harker diagrams suggest two populations: intermediate gneisses and volumetrically dominant acidic gneisses. Field evidence confirms that the intermediate gneisses are a minor component. The acidic gneisses are rhyolitic to dacitic in chemistry and in modal mineralogy (cf. Figure 4). The intermediate gneisses, although of dacitic modal mineralogy, feature SiO_2 analyses that are characteristic of andesites and are therefore interpreted as andesites. The intermediate gneisses contain more Fe_2O_3, MgO, MnO, TiO_2 and CaO than the acidic gneisses. Abundances of Al_2O_3, K_2O and Na_2O are comparable for both the intermediate gneisses and acidic gneisses. BH-INT also contains less total Rb and Sr than BH-ACID but has comparable Rb/Sr (BH-ACID, Rb/Sr = 0.04-1.10; BH-INT. Rb/Sr = 0.41-0.71). GBH is low in Na_2O, Sr, Ba and high in K_2O and Rb relative to BH-ACID. The vertical scatter of points on the SiO_2-K_2O and SiO_2-Na_2O diagrams

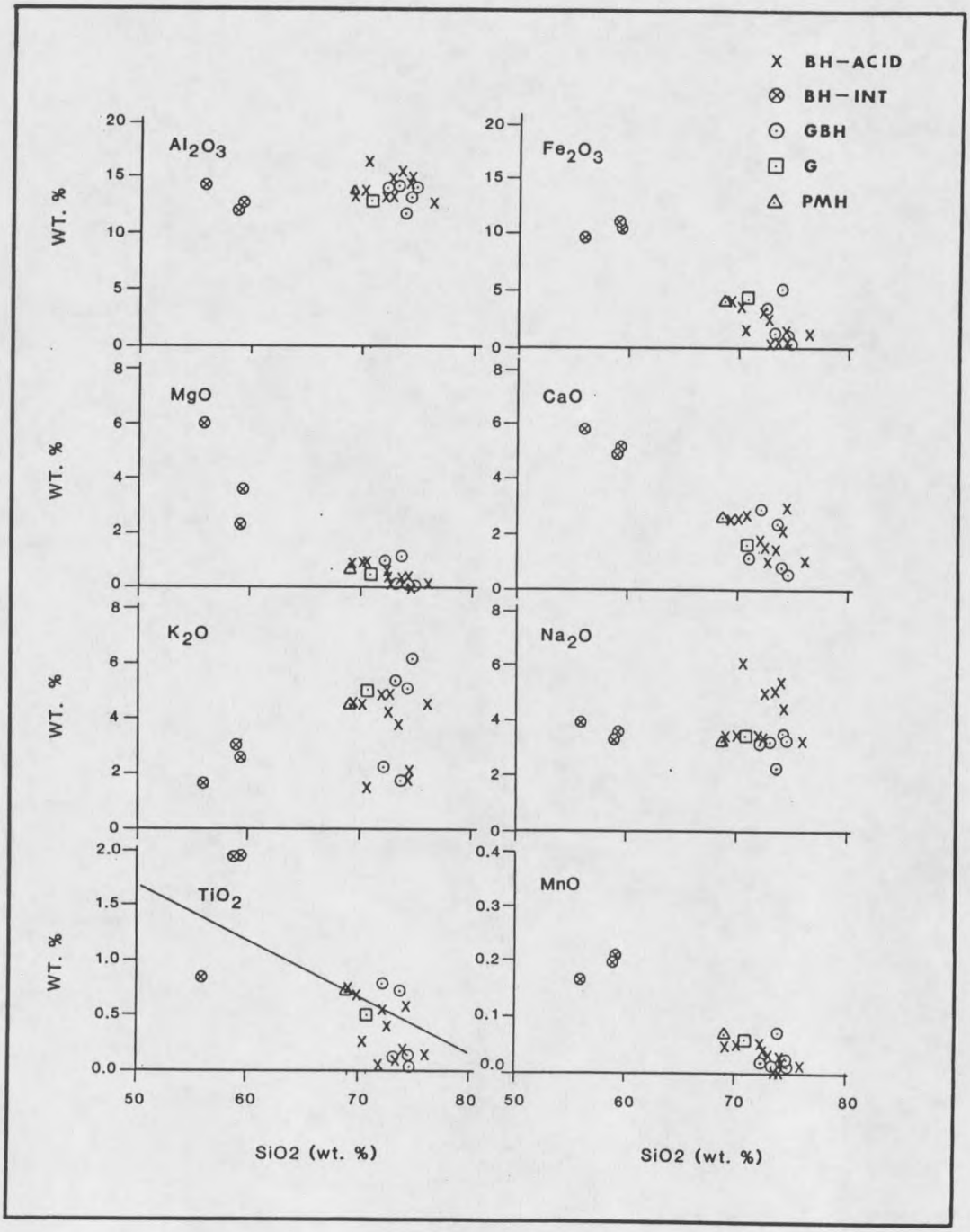

Figure 10. Felsic gneiss data for BH-ACID, BH-INT, GBH, PMH and G are plotted on Harker diagrams. Two populations are apparent: acidic gneisses and intermediate gneisses. The intermediate gneisses have silica values characteristic of andesites.

(Figure 10) is an effect of variations in the plagioclase and potassium feldspar modal mineralogy within the acidic gneisses (cf. Figure 4).The SiO_2-TiO_2 diagram is divided into igneous and sedimentary fields, after Tarney (1976). This division is based on samples of Archean and Phanerozoic rocks with known protoliths. Three of ten BH-ACID, two of three BH-INT and two of five GBH gneiss samples plot in the sedimentary field. Half of the BH samples and all of the GBH samples contain normative corundum (see Figure 11). PMH and G contain normative diopside. Samples with large amounts of normative corundum are interpreted to have sedimentary protoliths, whereas samples with large amounts of normative diopside are interpreted to have igneous protoliths.

The rare earth element (REE) plot (Figure 12) exhibits variable trace element contents for the different types of BH gneisses. Two dacite samples (BH-3, SiO_2 = 70.6 wt.% and BH-7, SiO_2 = 73.6 wt.%) show strong fractionation of light rare earth elements (LREE) over heavy rare earth elements (HREE), Ce/Yb = 19.2-26.4; and moderate positive Eu-anomalies, Eu/Eu* = 1.32-2.13. One rhyolite sample (BH-1, SiO_2 = 69.3 wt.%) shows moderate fractionation of LREE over HREE, Ce/Yb = 5.7; greater total REE contents than the dacite samples; and a slight negative Eu-anomaly, Eu/Eu* = 0.85. An andesite sample (BHM-3) contains more total REE than the BH-ACID samples and exhibits well-developed fractionation of LREE over HREE, Ce/Yb = 4.6; and a moderate negative Eu-anomaly, Eu/Eu* = 0.49. Protoliths of these REE samples are inferred to be volcanic rocks (discussed in detail in the PROTOLITH section of this study).

Table 3. Geochemical Analyses of Felsic Gneisses

Map Unit	BH-ACID							
Sample #	BH-1	BH-2	BH-3	BH-4	BH-5	BH-6	BH-7	BH-8
	MAJOR ELEMENT OXIDES (weight percent)							
SiO_2	69.3	70.3	70.6	72.3	72.6	72.9	73.6	74.3
Al_2O_3	13.5	13.6	16.4	13.1	13.1	14.7	15.3	14.6
CaO	2.49	2.59	2.59	1.75	1.59	1.01	1.49	2.08
MgO	0.87	0.82	0.87	0.51	0.30	0.01	0.26	0.37
Na_2O	3.36	3.33	6.04	3.31	3.29	4.89	4.97	5.26
K_2O	4.51	4.44	1.44	4.84	4.89	4.29	3.82	1.75
Fe_2O_3t*	4.05	3.70	1.54	2.96	2.40	0.47	0.56	1.30
MnO	0.05	0.05	0.01	0.05	0.04	0.03	<0.01	0.02
TiO_2	0.74	0.69	0.25	0.53	0.41	0.06	0.09	0.16
P_2O_5	0.20	0.18	0.09	0.13	0.10	0.04	0.03	0.03
LOI	0.54	0.47	0.47	0.47	0.70	0.85	0.31	0.31
SUM	99.9	100.4	100.5	100.2	99.7	99.4	100.7	100.3
K_2O/Na_2O	1.34	1.33	0.24	1.46	1.49	0.88	0.77	0.33
MgO+FeOt**	4.52	4.15	2.26	3.17	2.46	0.43	0.76	1.54
	TRACE ELEMENTS (parts per million)							
Rb	110	110	30	130	120	100	80	60
Sr	160	100	840	130	130	280	610	640
Y	40	50	10	40	40	10	<10	10
Zr	450	460	80	420	340	20	50	80
Nb	20	20	10	50	10	10	<10	10
Ba	1790	1510	660	1500	1750	560	1230	450
	CIPW Normative Minerals***							
Q	26.29	27.48	23.08	30.17	31.21	26.20	26.38	31.08
Or	27.33	26.68	8.60	29.09	29.55	25.74	22.55	10.40
Ab	29.16	28.66	51.64	28.50	28.48	42.02	42.02	44.78
An	8.65	9.20	12.39	6.71	6.68	4.82	7.19	10.18
Di	2.24	2.23		1.05	0.59			
Hy	2.09	1.88	1.90	1.47	1.08	0.19	0.59	1.03
C			0.83			0.55	0.70	0.69
Ap	0.45	0.40	0.20	0.29	0.23	0.09	0.07	0.07
Il	1.45	1.34	0.48	1.03	0.80	0.12	0.17	0.31
Mt	2.35	2.13	0.88	1.70	1.39	0.27	0.32	0.74
Hm								
Tn								
Wo								
total	100.00	100.00	100.00	100.00	100.00	100.00	100.00	100.00

*Total Fe was analyzed as Fe_2O_3.
**Total Fe is calculated as FeO.
***Calculated with $FeO/(FeO + Fe_2O_3) = 0.70$.

Table 3--Continued

Map unit	BH-ACID		BH-INT			GBH		
Sample #	BH-9	BH-10	BHM-1	BHM-2	BHM-3	GBH-1	GBH-2	GBH-3
	MAJOR ELEMENT OXIDES (weight percent)							
SiO_2	74.5	76.2	55.9	59.0	59.3	72.3	73.3	73.8
Al_2O_3	14.2	12.6	14.4	12.1	12.5	14.0	14.1	11.6
CaO	2.93	1.00	5.77	4.88	5.11	2.90	1.17	2.36
MgO	0.02	0.11	5.91	2.29	2.44	0.98	0.16	1.15
Na_2O	4.42	3.23	3.90	3.17	3.55	2.90	3.21	2.28
K_2O	2.03	4.52	1.66	3.03	2.62	2.27	5.37	1.77
Fe_2O_3t*	0.48	1.27	9.69	10.9	10.7	3.19	1.31	5.02
MnO	0.02	0.14	0.17	0.20	0.21	0.04	0.03	0.07
TiO_2	0.56	0.14	0.73	1.85	1.96	0.79	0.13	0.72
P_2O_5	0.02	0.05	0.11	0.62	0.65	0.12	0.04	0.12
LOI	0.39	0.85	1.77	0.93	0.62	0.54	0.31	0.39
SUM	99.7	100.2	100.1	99.3	100.0	100.4	99.4	99.5
K_2O/Na_2O	0.46	1.40	0.43	0.96	0.74	0.78	1.67	0.78
MgO+FeOt**	0.45	1.25	14.6	12.1	12.1	3.85	1.34	5.67
	TRACE ELEMENTS (parts per million)							
Rb	80	170	50	90	70	100	150	70
Sr	250	200	70	210	170	200	170	150
Y	80	10	10	100	100	50	20	50
Zr	360	190	110	990	860	1460	120	190
Nb	20	10	10	60	40	30	10	10
Ba	400	1520	430	1460	1220	1130	1470	1080
	CIPW Normative Minerals***							
Q	35.45	37.77	4.66	16.13	15.16	38.67	31.21	46.45
Or	12.06	26.91	10.75	18.99	16.22	13.46	32.01	10.67
Ab	37.63	27.54	36.18	28.45	31.48	24.64	27.41	19.69
An	12.99	4.67	18.51	10.44	10.93	13.66	5.59	11.15
Di	0.12		10.35	9.12	9.34			
Hy		0.61	11.75	5.15	5.11	2.39	0.72	3.51
C		1.40				3.59	1.97	3.94
Ap	0.04	0.11	0.27	1.45	1.50	0.27	0.09	0.27
Il	0.80	0.27	1.52	3.74	3.91	1.51	0.25	1.40
Mt		0.72	6.01	6.54	6.35	1.81	0.75	2.90
Hm	0.19							
Tn	0.36							
Wo	0.36							
total	100.00	100.00	100.00	100.00	100.00	100.00	100.00	100.00

*Total Fe was analyzed as Fe_2O_3.
**Total Fe is calculated as FeO.
**Calculated with $FeO/(FeO + Fe_2O_3) = 0.70$.

Table 3--Continued

Map Unit	GBH		PMH	G
Sample #	GBH-4	GBH-5	PMH-1	G-1
MAJOR ELEMENT OXIDES (weight percent)				
SiO_2	74.4	74.8	69.1	70.8
Al_2O_3	13.2	14.1	13.7	12.6
CaO	0.81	0.60	2.64	1.60
MgO	0.14	0.06	0.72	0.45
Na_2O	3.47	3.31	3.16	3.34
K_2O	5.11	6.18	4.40	5.10
Fe_2O_3t*	1.31	0.58	4.02	4.38
MnO	0.04	0.03	0.07	0.06
TiO_2	0.15	0.04	0.71	0.50
P_2O_5	0.04	0.06	0.20	0.10
LOI	0.39	0.31	0.16	0.16
SUM	99.2	100.1	99.2	99.4
K_2O/Na_2O	1.47	1.87	1.39	1.53
MgO+FeOt**	1.32	0.58	4.34	4.39
TRACE ELEMENTS (parts per million)				
Rb	330	120	110	200
Sr	50	10	150	80
Y	70	10	40	90
Zr	130	20	550	530
Nb	20	20	30	40
Ba	500	170	1750	1540
CIPW Normative Minerals***				
Q	32.79	30.32	27.50	27.71
Or	30.62	36.34	26.79	30.95
Ab	29.78	27.88	27.56	29.03
An	3.81	2.57	10.52	4.44
Di			1.36	2.47
Hy	0.68	0.32	2.09	1.64
C	1.18	2.03		
Ap	0.09	0.13	0.45	0.23
Il	0.29	0.08	1.39	0.98
Mt	0.75	0.33	2.34	2.55
Hm				
Tn				
Wo				
total	100.00	100.00	100.00	100.00

*Total Fe was analyzed as Fe_2O_3.
**Total Fe is calculated as FeO.
***Calculated with $FeO/(FeO + Fe_2O_3) = 0.70$.

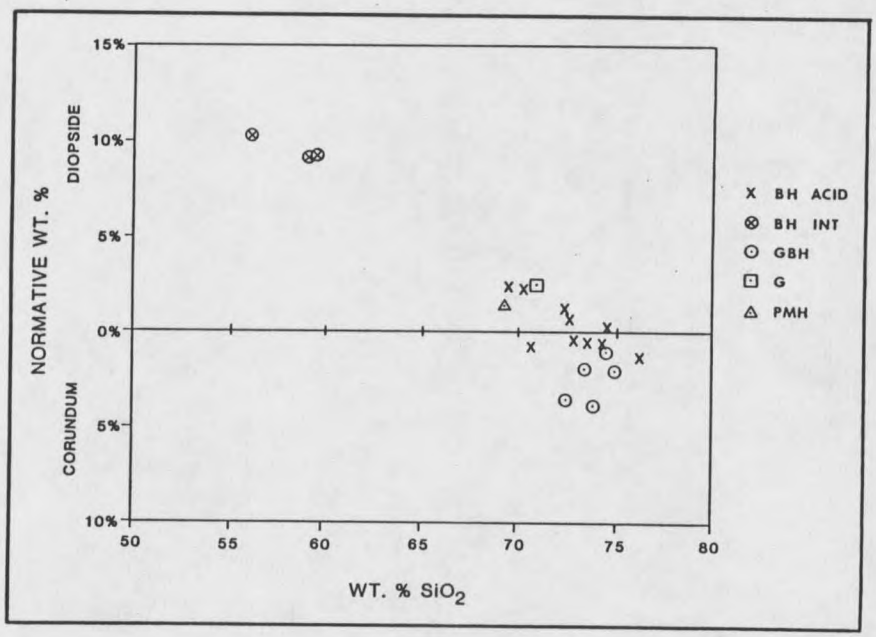

Figure 11. Abundances of mutually exclusive normative diopside and normative corundum are compared to wt.% SiO_2 for all felsic gneisses.

Generation of melts with REE patterns of the dacite samples (BH-3 and BH-7)--characterized by positive Eu-anomalies, low-to-moderate total REE contents, and large LREE/HREE ratios--requires either, a) partial melting of an amphibolite, eclogite, or garnet-amphibolite source, or b) crystal fractionation of hornblende and/or garnet from a melt of more basic composition (Hanson, 1980; Cullers and Graf, 1984). If crystal fractionation were involved, and if the volcanic rocks were extruded periodically from the magma chamber during fractionation, comparable volumes of intermediate through acidic volcanic rocks should be preserved. Moreover, intermediate volcanic rocks that belong to the differentiating series should have REE contents intermediate between the acidic and basic end-members of the series. However, the sequence

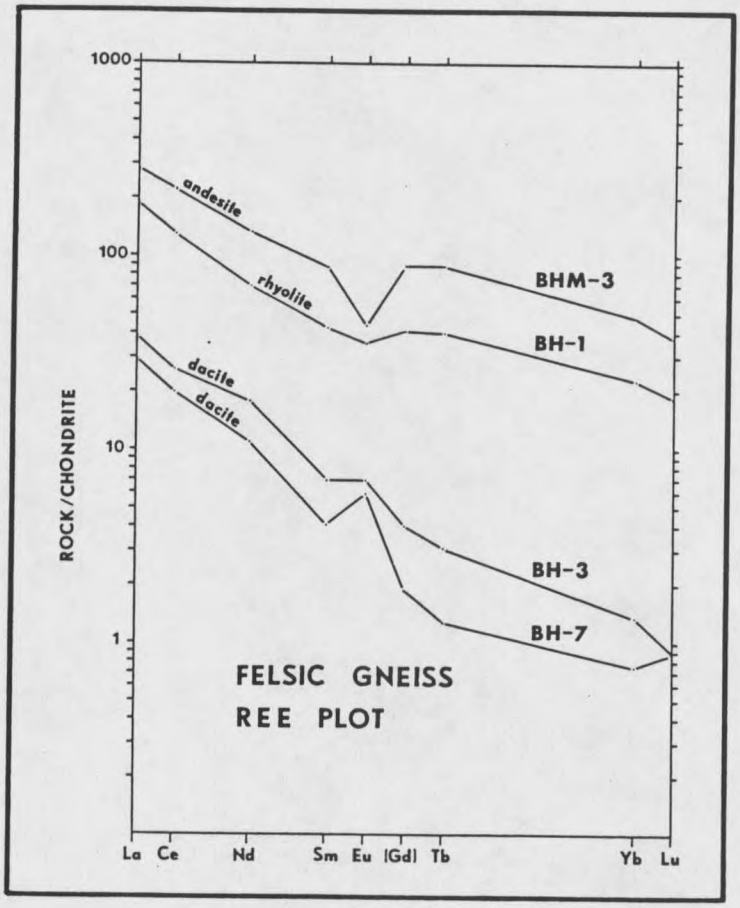

Figure 12. Rare earth element (REE) abundances, normalized to chondrite values, are plotted for three BH-ACID samples (two dacites and one rhyolite) and one BH-INT sample (an andesite).

in the Blacktail Mountains is dominated by acidic gneisses, and includes only minor volumes of intermediate gneiss. Furthermore, the intermediate gneiss that was analyzed contains greater amounts of REE than any of the acidic gneisses, and could not have been part of a fractionating sequence. Consequently, the parent melt of the volcanic rocks could not have been generated by fractional crystallization. Alternatively, partial melting of an amphibolite, eclogite or garnet-amphibolite source can produce dominantly acidic volcanic rocks with

the observed REE patterns, without producing significant volumes of intermediate volcanic rocks. Hence, partial melting of a mafic source is accepted as the best model for the generation of the dacite samples (BH-3 and BH-7).

Generation of a melt with the REE pattern of the rhyolite sample (BH-1)--characterized by a small negative Eu-anomaly and moderate total REE contents--is possibly an effect of partial melting of sialic material (including metasediments and/or granitoid plutons), with abundant plagioclase remaining in the residue. Alternatively, the pattern may be generated by fractional crystallization of abundant plagioclase and small amounts of minerals such as sphene, allanite, hornblende or apatite from a more basic melt (Hanson, 1980; Cullers and Graf, 1984). Generation of the REE pattern by fractional crystallization is considered untenable based on the same arguments presented for the REE patterns of the dacite samples. Therefore, the preferred model for generation of this rhyolite sample is partial melting of pre-existing continental crust.

Generation of a melt with the REE pattern of the andesite sample (BHM-1) is problematic. The high total REE content and the moderate negative Eu-anomaly are unusual for an andesite (Cullers and Graf, 1984). The pattern may be an effect of hydrothermal alteration, or it may represent the REE content of an unaltered sample. If the pattern does represent an unaltered sample, then a complex history of multi-stage partial melting and crystal fractionation may be invoked to account for the high total REE content and the negative Eu-anomaly

(Cullers and Graf, 1984). Alternatively, this andesite may have been generated from a REE-enriched mantle source (e.g., Mueller and others, 1983).

Mafic Rocks

Major element oxide, trace element and normative mineralogy data for the mafic rocks are presented in Table 4. The alkalic/subalkalic character of the mafic rocks is illustrated by samples plotted on the SiO_2-alkalis diagram in Figure 13. All amphibolite, ultramafite, and gabbroic dike samples and one granulite sample plot in the subalkalic field. One granulite sample (GB-1) plots in the alkalic field. The mafic rocks that plot in the subalkalic field contain normative hypersthene-olivine or hypersthene-quartz (refer to Table 4). The granulite sample which plots in the alkalic field contains normative

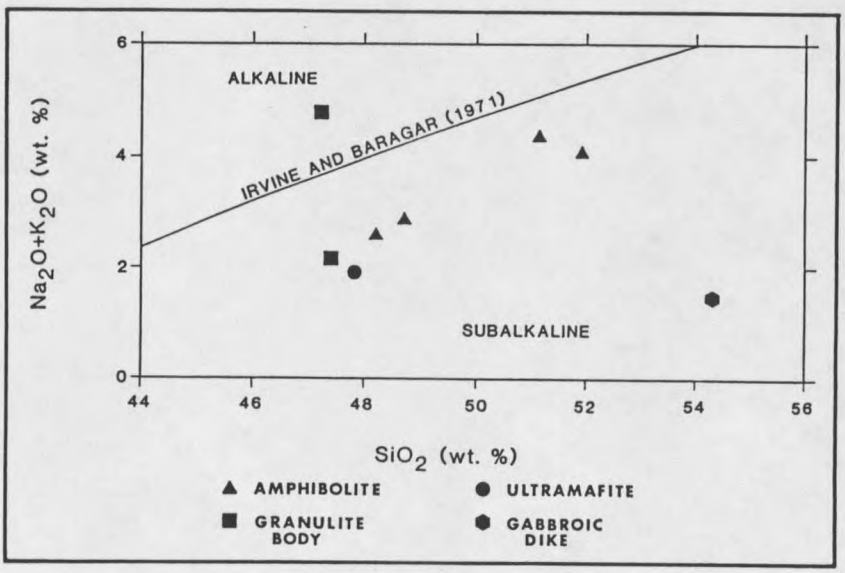

Figure 13. Total alkali content is plotted against wt.% SiO_2 to distinguish between alkalic and subalkalic affinities for the mafic rocks.

hypersthene-olivine. Although sample GB-1 plots in the alkalic field (Figure 13), it does not contain characteristic normative alkalic minerals (nepheline or leucite) and it may be transitional. Alternatively, sample GB-1 may have been affected by later alteration.

The tholeiitic/calc-alkalic nature of the mafic rocks is reflected in the AFM diagram of Figure 14. All mafic rock and felsic gneiss samples are plotted. Two amphibolite and two granulite samples and the single ultramafite and gabbroic dike samples plot above the tholeiitic/calc-alkalic boundary of Irvine and Baragar (1971). Two amphibolite samples plot below this boundary. The small mafic rock

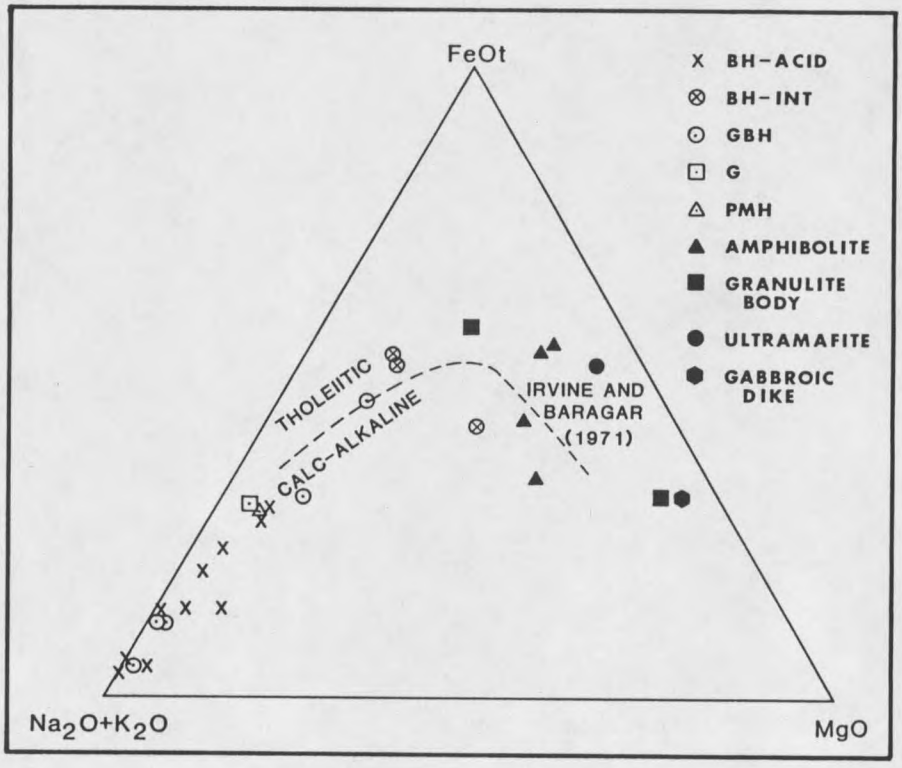

Figure 14. All felsic gneiss and mafic rock samples are plotted on an AFM diagram. The pattern has both tholeiitic and calc-alkalic characteristics. The tholeiitic/calc-alkalic field boundary is from Irvine and Baragar (1971).

sample population inhibits clear recognition of a tholeiitic or calc-alkalic trend. However, a tholeiitic trend may be defined by two of four amphibolite samples (A1 and A2), the two granulite and two of three BH-INT samples. A calc-alkalic trend is suggested by two other amphibolite samples (A3 and A4) and one of three BH-INT samples. Samples plotted on the AFM diagram seem to have tholeiitic and calc-alkalic characteristics.

Irvine and Baragar (1971) successfully discriminated between tholeiitic and calc-alkalic Cenozoic basalts using Al_2O_3 content. The mafic rocks of the Blacktail Mountains are plotted on an Al_2O_3-plagioclase diagram in Figure 15 (from Irvine and Baragar, 1971). The

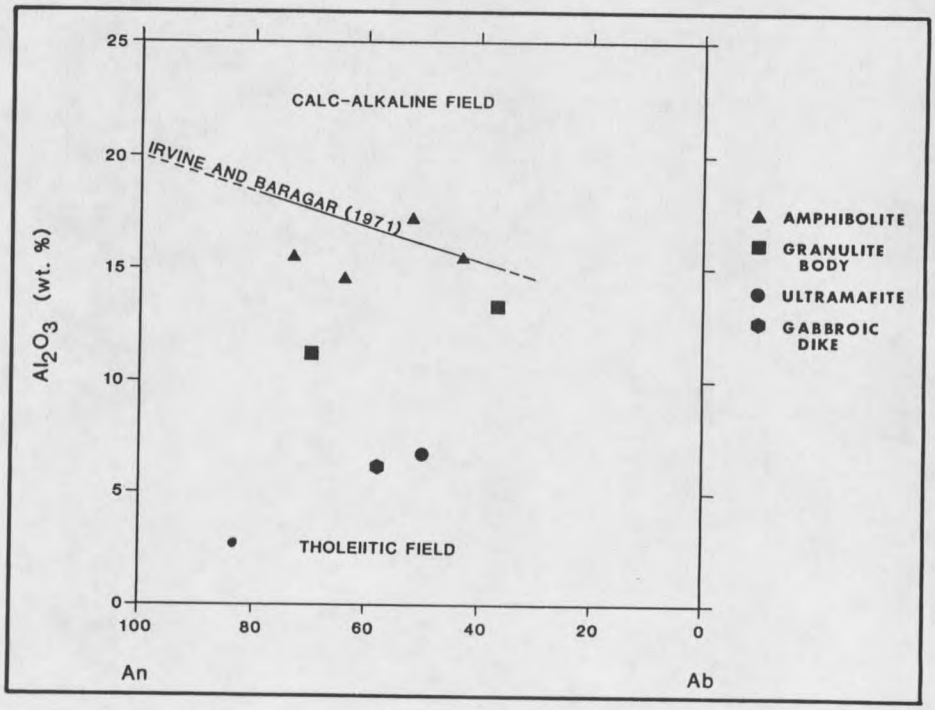

Figure 15. Normative plagioclase composition is plotted against Al_2O_3 contents of the mafic rocks to further identify tholeiitic or calc-alkalic characteristics (from Irvine and Baragar, 1971).

2 samples (A-3 and A-4) that show calc-alkalic affinities on the AFM diagram also show calc-alkalic affinities on the Al_2O_3-plagioclase diagram. The remainder of the mafic rocks plot in the tholeiitic field, which is consistent with the AFM diagram. Mafic rocks of the Blacktail Mountains appear to be dominantly tholeiites with some calc-alkalic varieties. However, a tholeiitic suite may exhibit calc-alkalic chemistry as a result of hydrothermal activity (MacGeehan and MacLean, 1980) or retrograde metamorphism of granulite-grade rocks (Beach and Tarney, 1978).

REE data for an amphibolite sample (A-1) and a granulite sample (GB-1) are plotted in Figure 16. The amphibolite has an unfractionated REE curve and is moderately enriched in total REE (REE = 10-22 x chondrite). Data for the granulite sample show fractionation of LREE/HREE (Ce/Yb = 5.2) and strong enrichment of total REE (Ce = 195 x chondrite). The granulite-sample curve also shows a moderate negative Eu-anomaly (Eu/Eu* = 0.72). The elevated REE values for the granulite sample are enigmatic and may be the result of assimilation of sialic material with a low fusion temperature and a high concentration of incompatible elements (Barley, 1986). This granulite sample (GB-1) is enriched in the incompatible elements Y, Zr, and Ba compared to the other granulite sample (GB-2).

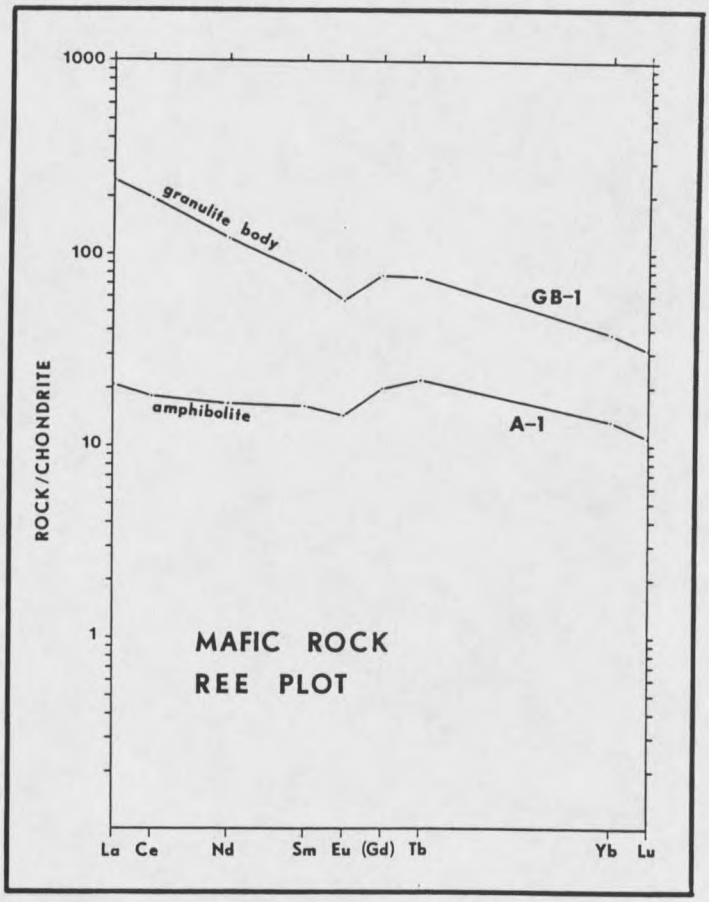

Figure 16. Rare earth element abundances, normalized to chondrite values, are plotted for an amphibolite sample and a granulite sample.

Table 4. Geochemical Analyses of Mafic and Ultramafic Rocks

	Amphibolite				Granulite Bodies		UM	GD
Sample #	A-1	A-2	A-3	A-4	GB-1	GB-2	UM-1	GD-1
				Major Element Oxides (weight percent)				
SiO_2	48.2	48.7	51.1	51.9	47.2	47.4	47.8	54.3
Al_2O_3	14.5	15.5	15.4	17.2	13.3	11.2	6.76	6.11
CaO	11.0	8.19	9.10	11.5	7.63	7.58	10.6	5.21
MgO	7.46	6.71	7.23	7.03	4.88	17.4	11.8	19.5
Na_2O	1.95	1.38	3.63	3.28	3.40	1.15	1.30	0.93
K_2O	0.59	1.48	0.71	0.81	1.36	0.99	0.60	0.55
Fe_2O_3t*	14.2	12.9	9.89	6.65	15.6	10.5	17.1	11.3
MnO	0.22	0.18	0.14	0.15	0.19	0.16	0.23	0.19
TiO_2	1.17	1.46	1.06	0.20	2.70	0.66	1.70	0.49
P_2O_5	0.11	0.21	0.21	0.04	1.09	0.14	0.16	0.07
LOI	0.47	2.85	0.85	0.85	1.62	1.08	0.31	0.08
SUM	100.0	99.6	99.4	99.7	99.2	98.6	98.5	99.1
Mg'**	0.51	0.51	0.59	0.68	0.38	0.77	0.58	0.78
				Trace Elements (parts per million)				
Cr	270	90	220	20	110	2130	680	2480
Rb	30	60	10	10	50	50	20	30
Sr	160	150	310	250	150	90	80	40
Y	20	20	10	<10	60	20	20	20
Zr	50	70	90	10	690	70	70	70
Nb	<10	10	20	20	40	20	40	20
Ba	310	310	290	100	800	280	350	250
				CIPW Normative Minerals***				
Q		5.24						6.01
Or	3.75	10.01	4.33	4.75	8.72	6.21	3.95	4.07
Ab	17.76	13.37	31.73	27.54	31.21	10.33	12.24	9.85
An	31.29	36.34	24.41	29.59	18.46	23.86	12.06	13.62
Di	22.76	7.37	17.94	23.20	12.57	13.21	38.99	15.92
Hy	11.86	15.58	6.73	2.72	8.70	16.56	17.81	41.17
Ol	1.28		6.51	8.01	2.59	21.87	0.81	
C								
Ap	0.26	0.53	0.48	0.09	2.60	0.33	0.39	0.19
Il	2.40	3.18	2.08	0.38	5.58	1.33	3.60	1.17
Mt	8.65	8.36	5.78	3.73	9.58	6.31	10.77	8.01
total	100.00	100.00	100.00	100.00	100.00	100.00	100.00	100.00

*total Fe was analyzed as Fe_2O_3.
**Mg' (magnesium number) = mols MgO/(mols MgO + mols FeOt)
***calculated with $FeO/(FeO + Fe_2O_3) = 0.70$

CHAPTER 7

PROTOLITH

Felsic Gneisses

Protolith determination of the felsic gneisses must reconcile both lithologic and geochemical lines of evidence. Although primary igneous textures may be obliterated during a high-grade, tectonothermal event, general lithologic relationships that may characterize a sequence can survive. Characteristics of compositional zonation within the Archean felsic gneisses of the Blacktail Mountains are reviewed in the following text. Afterward, geochemical characteristics that discriminate between plutonic and supracrustal protoliths for these felsic gneisses are evaluated. Lastly, results of lithologic and geochemical analyses are compared in order to best deduce the nature of the protolith.

Lithologic relationships and petrographic evidence are more consistent with a supracrustal protolith than a plutonic protolith. Cross-cutting relationships, xenoliths, or other textures that are characteristic of a plutonic protolith were not observed. High-grade metamorphism commonly obliterates primary igneous textures and the lack of such textures does not necessarily preclude a plutonic protolith. However, the features previously discussed in the LITHOLOGIES chapter of this study and reviewed below are more accordant with a supracrustal protolith than a plutonic protolith. All map units were observed to

have well-developed foliation and millimeter- to meter-scale compositional layering. Adjacent layers of differing mineralogy and of differing color index typically have gradational contacts. GBH includes layers (5-20 centimeters thick) which contain greater than 30% garnet. Map units BH, GBH, PMH and G are locally interlayered on a meter-scale, especially at their map boundaries. The GBH unit is host to several 5-20 meters-thick layers of marble and calc-silicate gneiss in the southeastern portion of the map area. Layers of G and BH (5-40 meters thick) and amphibolite layers (0.5-3 meters thick) are intercalated with marble-bearing GBH horizons. The presence of conformable marble layers is strong evidence for a supracrustal protolith for at least the marble-bearing GBH gneisses. The conformable and intimate interlayering of BH and G gneisses with GBH gneisses and the layering characteristics of BH suggest that these gneisses also have a supracrustal heritage. The layering characteristics featured by PMH gneisses suggest that this unit also had a supracrustal protolith.

Geochemical analyses, however, suggest a dominantly igneous protolith. Many methods of protolith discrimination have been studied and the methods which have yielded the most definitive results are presented in the following paragraphs and attendant diagrams (Figures 17-20). In Figure 17, data are plotted in terms of Niggli-c and Niggli-al-alk (Leake and Singhe, 1986), and produce a discrimination independent of silica content. A positive correlation indicates an igneous protolith, whereas a negative correlation indicates a sedimentary protolith. This diagram is best suited for QFGs composed

almost entirely of quartz and feldspar; wherein Niggli-al, -alk and -c reflect feldspar composition. The Niggli-al-alk axis is ideally (where quartz, plagioclase and potassium feldspar comprise 100 percent of the rock) a measure of Al_2 in anorthite. The Niggli-c axis is ideally a measure of Ca in anorthite. A line with slope = 1 (the An-line) is a measure of anorthite content in plagioclase. Potassium feldspar, albite and quartz plot at the origin. Since the compositions of nearly

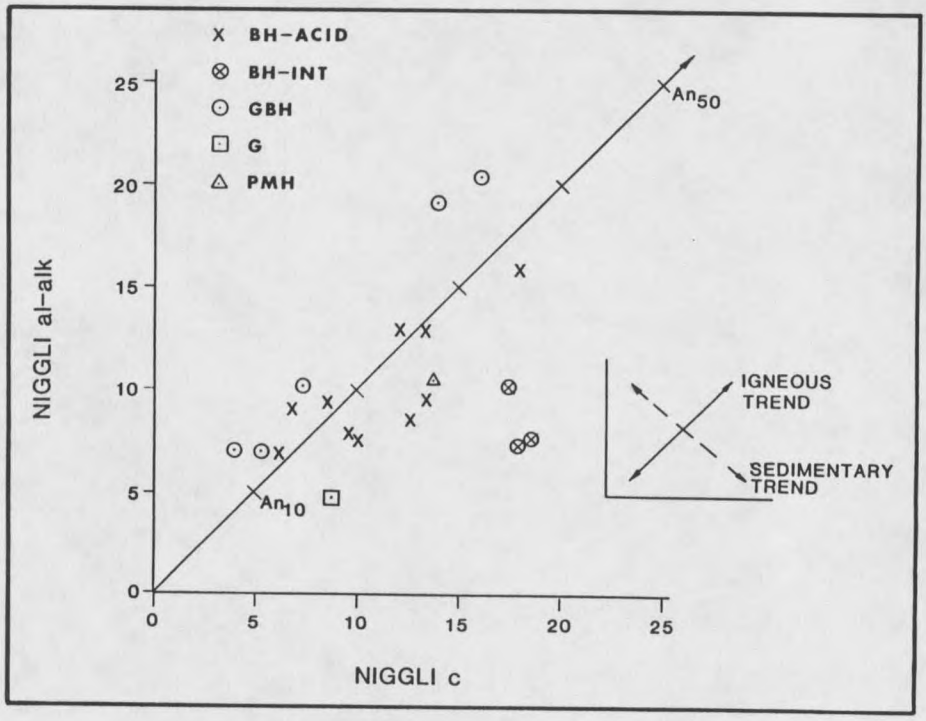

Figure 17. Niggli-c values are plotted against Niggli-al-alk values for all felsic gneisses. Positive correlations indicate igneous parent rocks. Negative correlations indicate sedimentary parent rocks (Leake and Singh, 1986).

all igneous series increase in potassium feldspar, quartz and albite and decrease in anorthite with increasing differentiation, typical igneous differentiation trends are represented by the An-line. Clays,

constituents of shales, are rich in Niggli-al-alk, deficient in Niggli-c and plot left of the An-line. Dolomites and limestones are rich in Niggli-c and devoid of Niggli-al-alk and plot to the right of the An-line, on the abscissa. Quartz arenite and arkose are dominated by quartz and feldspars, and overlap the An-line. Shales, sandstones and carbonates are commonly interlayered in the sedimentary record and samples from a suite of these lithologies would plot orthogonal to the An-line. Data for the Archean sequence in the Blacktail Mountains show a strong positive correlation of Niggli-al-alk vs. Niggli-c, and indicate an igneous protolith.

In Figure 18, data are plotted in terms of Niggli-mg vs. Niggli-si (Van de Kamp and others, 1975; Leake and Singh, 1986). A negative correlation indicates igneous parentage and reflects generally decreasing amounts of Mg-bearing minerals and decreasing Mg/Fe ratio with increasing silica content. However, a negative correlation may also reflect the compositional maturity of sediment. For example, Mg-bearing micas and clays may be present in immature sediments and may be winnowed out as silica is concentrated. A wide scatter and/or a positive correlation generally indicates sedimentary parent rocks. Data are somewhat scattered, but plot with a generally negative correlation and indicate either an igneous or a compositionally immature clastic protolith.

In Figure 19, samples are distinguished between meta-igneous rocks and metasedimentary rocks by plotting data in the ternary system CaO-MgO-Al_2O_3 (Leyreloup and others, 1977). This diagram provides another discrimination independent of silica content. Data which plot in the

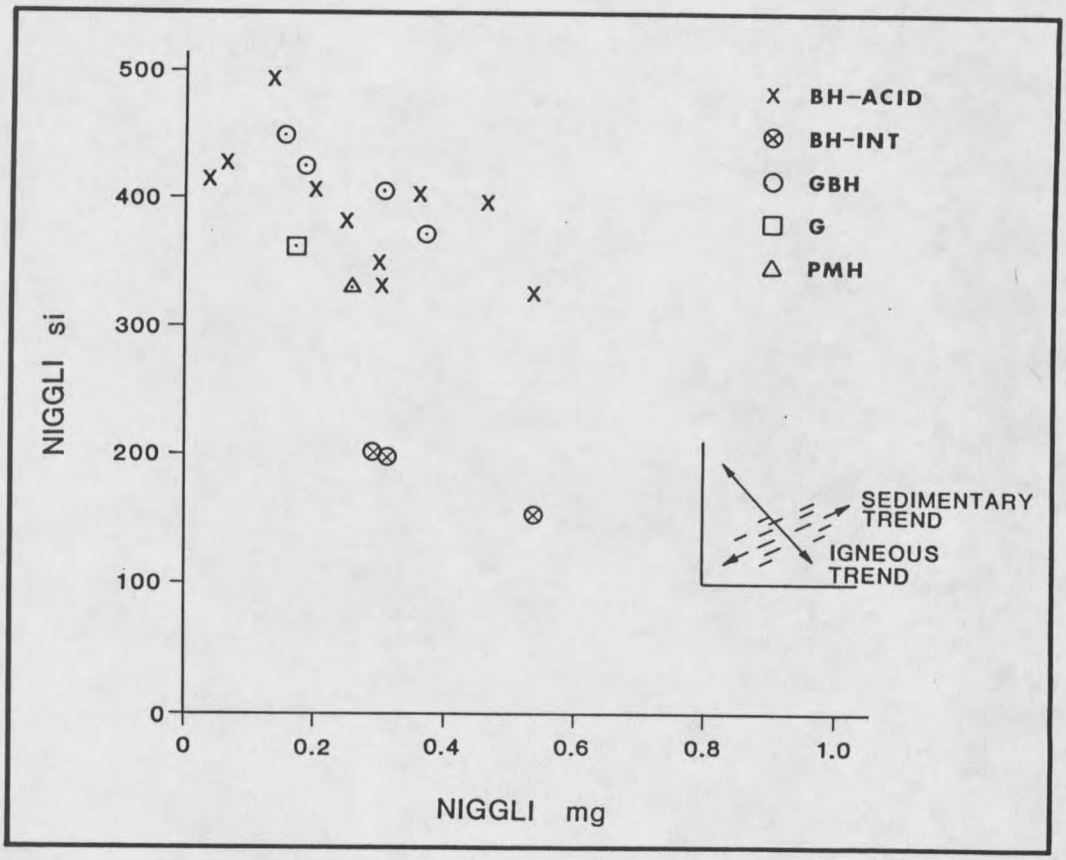

Figure 18. Niggli-si values are plotted against Niggli-mg values for all felsic gneiss samples. Negative correlations indicate igneous parent rocks. Positive or dispersed correlations indicate sedimentary parent rocks (Van de Kamp and others, 1975; Leake and Singh, 1986).

igneous field reflect the varying abundance of Ca-Al-Mg in mafic minerals and Al-Ca in anorthite. The sedimentary field reflects the disintegration of anorthite, least stable of the feldspars at surface conditions, and the loss of CaO due to weathering. Data for samples from the Blacktail Mountains plot along the meta-igneous/metasedimentary boundary. This pattern is consistent with an igneous differentiation trend, wherein abundances of MgO and CaO decrease and Al_2O_3 increases with increasing differentiation.

Distribution of data along the meta-igneous/ metasedimentary boundary indicates either fortuitous compositions of unaltered igneous rocks or igneous rocks of a series that have been slightly reworked by sedimentary processes.

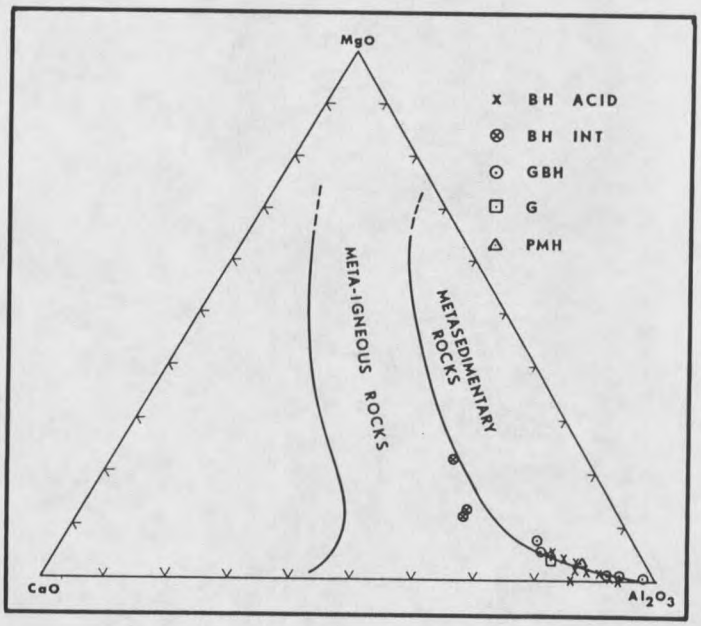

Figure 19. CaO-MgO-Al_2O_3 contents of the felsic gneisses plot along the line separating the metasedimentary and meta-igneous fields (from Leyreloup and others, 1977).

In Figure 20, data are plotted in terms of the igneous-sedimentary discriminant function of Shaw (1972) vs. alkali ratio. Shaw's discriminant function is of the following form (coefficients are multiplied by wt.% oxide):

$$DF3 = 10.44 - 0.21SiO_2 - 0.32Fe_2O_3t - 0.98MgO + 0.55CaO + 1.46Na_2O + 0.54K_2O.$$

Positive values of DF3 indicate igneous parentage and negative values indicate sedimentary parentage. High concentrations of SiO_2 coupled

with high concentrations of Fe_2O_3 and MgO contribute to a negative value of DF3. This is consistent with positive correlations of SiO_2 vs. MgO and SiO_2 vs. Fe_2O_3, which indicate a sedimentary parent rock (Van de Kamp and others, 1975; Leake and Singh, 1986). High concentrations of CaO, Na_2O and K_2O reflect the presence of unweathered feldspars. Most samples of felsic gneisses from the Blacktail Mountains plot in the positive field, and apparently have igneous parent rocks. One GBH and one BH-INT sample plot in the negative field, characteristic of sedimentary parentage. Na_2O-rich samples of acidic gneisses are more strongly positive than K_2O-rich acidic gneiss samples. This variation in alkali content may be an effect of weathering of the protoliths of the acidic gneisses. Na_2O is partitioned into seawater much more strongly than K_2O (Whitfield and Turner, 1979; Taylor and McLennan, 1985). Weathering processes may have removed Na_2O and concentrated K_2O and may be responsible for the trend observed in Figure 20. GBH samples are also generally less strongly positive than BH-ACID samples, a possible effect of removal of CaO, Na_2O and K_2O by weathering. Alternatively, the patterns may simply be effects of hydrothermal alteration of the parent rock.

Field evidence indicates a supracrustal protolith while the geochemical evidence suggests an igneous protolith. A locally reworked volcanic protolith is compatible with both lines of reasoning. Alternatively, the protolith could have consisted of compositionally immature clastic sediments that were eroded from plutons of granitic to tonalitic composition and deposited into an adjacent basin. Rapid

erosion, deposition and burial might have preserved the igneous-geochemical signatures of such sediments. However, a protolith of compositionally immature clastic sediment is unlikely because an older granite (senso stricto) sediment source (older than the 3.08 Ga age assigned to the sequence in the Blacktail Mountains (Giletti, 1966)); which is required for the potassium feldspar-rich felsic gneisses; is

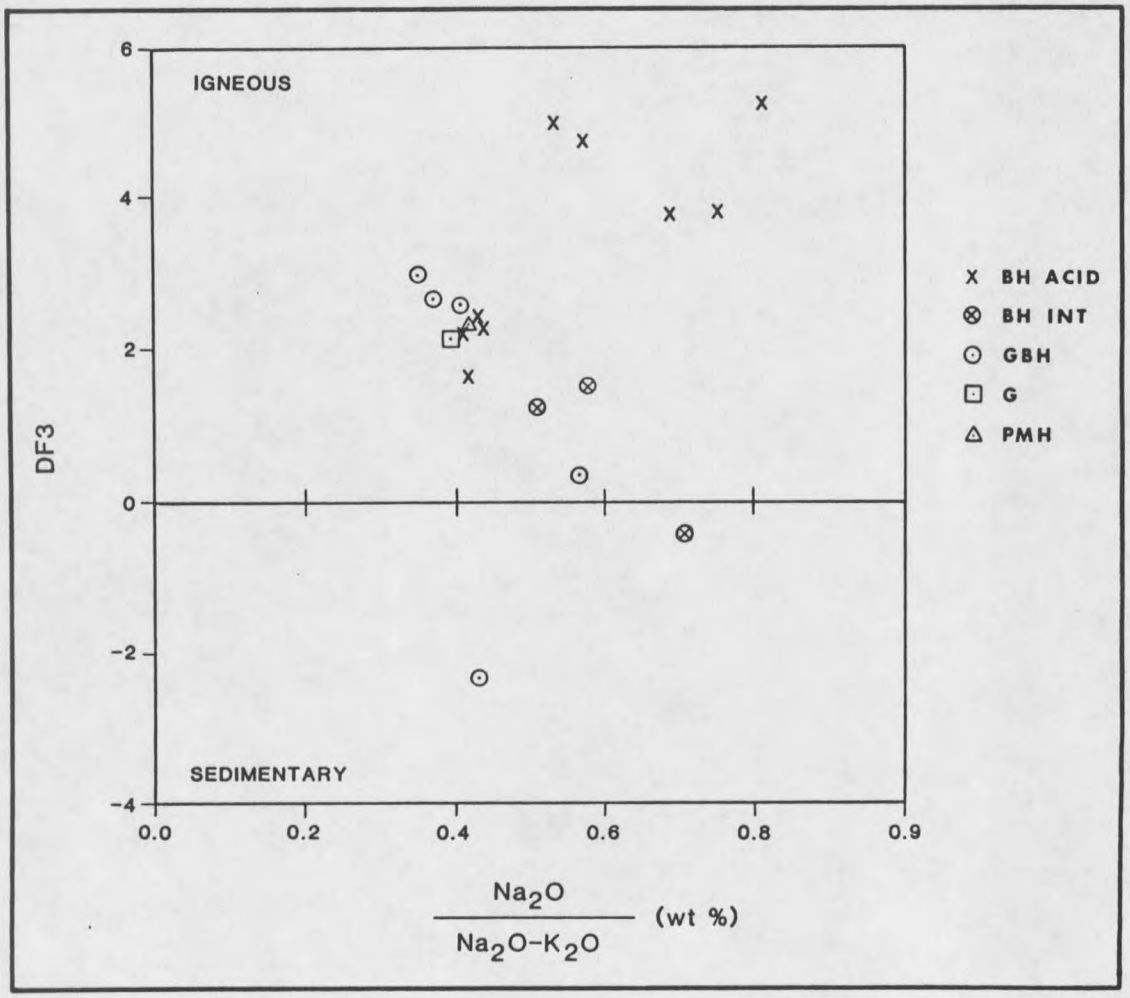

Figure 20. Multivariable discriminant function values, DF3, of Shaw (1972) plotted against alkali ratio distinguish between igneous and sedimentary parent rocks and illustrate variations in alkali ratios.

not recognized in the region. Furthermore, granite (senso stricto) plutons were not common in Archean terranes throughout the world until latest Archean time (e.g., Windley, 1984). Moreover, features associated with immature clastic sedimentation that may be preserved after high-grade metamorphism, such as compositional domains representing coarse conglomerates, are not observed. Consequently, a protolith composed of compositionally immature clastic rocks is considered unlikely. Alternatively, a volcanic protolith is the most direct interpretation of the geochemical discrimination. Moreover, a volcanic protolith is consistent with the observed bimodal rhyolite/dacite-basalt characteristics of the sequence. The protolith of the BH gneisses (including both BH-ACID and BH-INT) was most likely composed of volcanic and volcaniclastic rocks.

The GBH gneisses are modeled as BH volcanics that have been reworked to concentrate enough aluminum relative to other constituents to grow garnets. The relative enrichment of K_2O and depletion of Na_2O in GBH gneisses relative to BH gneisses is compatible with reworking by water and may be the result of selective solution of Na_2O in water and concentration of K_2O in clay minerals (see Table 3). Aluminum tends to stay at the weathering site in the form of clay minerals (Brownlow, 1979). Al_2O_3 contents in the BH gneisses and GBH gneisses are comparable (see Figure 10), and are consistent with reworking of BH-protolith sediments to form GBH-protolith sediments. Alternatively, the enrichment of K_2O relative to Na_2O may be an effect of potassic alteration related to hydrothermal activity (e.g., Nutman and others, 1984). The trend on Figure 11, which shows decreasing abundances of

normative diopside and increasing abundances of normative corundum with progressive change from BH to GBH, is also compatible with a transition from BH to GBH protoliths due to weathering. The discriminant function of Shaw (1972) plotted against alkali ratio (see Figure 20) shows a trend of increasing sedimentary affinities with decreasing $Na_2O/(Na_2O+K_2O)$. This trend is also compatible with the proposed relationships of the BH and GBH protoliths. Marbles are present where the GBH unit is thickest. Marbles are characteristically subaqueous deposits. The association of marble layers with the thickest section of GBH indicates that a body of water was probably involved in the weathering and alteration of BH-protolith sediments to GBH-protolith sediments.

Mafic and Ultramafic Rocks

The mafic rocks of the Blacktail Mountains; including amphibolites, granulites, ultramafites and gabbroic dikes; may be regarded as basalts derived from the upper mantle (Carmichael and others, 1974). The mafic and ultramafic rocks were characterized in Chapter 6 of this study. Protoliths of the amphibolites were characterized as basalts with tholeiitic and calc-alkalic affinities. Protoliths of the granulite samples were regarded as tholeiitic basalts, although one sample (GB-1) was considered to be transitional between alkalic and subalkalic basalts. The ultramafite and gabbroic dike samples were also regarded as tholeiitic basalts. The origins of the mafic and ultramafic rocks are discussed below.

Chemical characteristics of the amphibolites; 6.71-7.46 wt.% MgO, 6.65-14.2 wt.% Fe_2O_3t, 8.19-11.5 wt.% CaO, 2.86-4.34 wt.% total alkalis and Mg' = 0.51-0.68; suggest derivation of these units from partial melting of a mantle source, with minimal contamination from sialic material during emplacement (Basaltic Volcanism Study Project, 1981). One amphibolite sample (A-4) contains greater Al_2O_3 (17.2 wt. %) than the other amphibolites, and may have been contaminated with sialic material during its emplacement. The amphibolite-sample REE pattern (see Figure 16) is compatible with that of a melt derived from partial fusion (5-8% melting) of garnet lherzolite mantle (Hanson, 1980).

One granulite body (sample GB-1) has the chemistry of iron-rich basalts (Basaltic Volcanism Study Project, 1981); high Fe_2O_3t (15.6 wt.%), total alkalis (4.76 wt.%) and TiO_2 (2.70 wt.%). The REE pattern of this granulite (see Figure 16) is of problematic origin and may represent a melt derived from a mantle or basalt parent and subsequently contaminated with low-fusion temperature sialic material during emplacement (Barley, 1986), or from an enriched mantle source (Mueller and others, 1983).

The chemistry of another granulite body (sample GB-2); very high MgO (17.4 wt.%), Cr (2130 ppm) and Mg' (0.77); is similar to basaltic komatiites (Basaltic Volcanism Study Project, 1981). Archean basaltic komatiites typically occur as layers in greenstone belts, and are thought to be generated according to one of two models: 1) high degree of partial melting of mantle pyrolite under conditions of unusually high geothermal gradients (Green, 1975), or 2) much lower degree of partial melting of a magnesium-rich, refractory mantle diapir under

conditions of much lower geothermal gradients (McKenzie and Weiss, 1975). Weaver and Tarney (1979) and the Basaltic Volcanism Study Project (1981) favor komatiite origin by partial melting of a magnesium-rich, refractory mantle diapir in order to avoid the requirement of an unusually high geothermal gradient.

The chemistry of the ultramafite sample is that of a high-magnesian basalt (Basaltic Volcanism Study Project, 1981); high MgO (11.8 wt.%), low total alkalis (1.90 wt.%), high Cr (680 ppm), and Mg' = 0.58. Ultramafite bodies are concordant to compositional layering in the host felsic gneisses, are coarse grained, and are unfoliated to poorly foliated. The origin of the ultramafites is uncertain, but possibilities include an injected ultramafic liquid or tectonically emplaced mantle remnants. The small volumes of ultramafite and lack of recognized ocean-crust remnants in similar terranes of the Ruby Range (e.g., Desmarais, 1981) suggest that the ultramafites in the Blacktail Mountains may have been emplaced as sills.

The gabbroic dike sample is similar in chemistry to basaltic komatiites (Basaltic Volcanism Study Project, 1981); very high MgO (19.5 wt.%), Cr (2480 ppm) and Mg' (0.78). However, the sample contains unusually high SiO_2 (54.3 wt.%) relative to its primitive high Mg', and may have been re-silicified after its emplacement. The dikes are west- to northwest-trending, unfoliated and are strongly discordant to compositional layering in the felsic gneisses. Gabbroic dikes of the Blacktail Mountains are similar in orientation to diabase dikes in the Ruby and Tobacco Root ranges, which are almost exclusively west- to northwest-trending and strongly discordant to Archean lithologies

(Wooden and others, 1978; Karasevich and others, 1981). Some of these dikes have been dated as late Proterozoic (Wooden and others, 1978). All west- to northwest-trending diabase dikes in the Ruby and Tobacco Root ranges are inferred to be similar in age to those that have been dated, and have been associated with extensional tectonics related to opening of the Belt Basin (Schmidt and Garihan, 1986). The west- to northwest-trending gabbroic dikes of the Blacktail Mountains are also inferred to be late Proterozoic in age, solely on the basis of similar orientation. Emplacement of these dikes may also have been an effect of extensional tectonics related to opening of the Belt Basin. However, the basaltic komatiite chemistry of the gabbroic dike sample (19.5 wt.% MgO) is unique compared to the basaltic chemistry of diabase dike samples (3-9 wt.% MgO) from the Ruby and Tobacco Root ranges (Wooden and others, 1978).

CHAPTER 8

TECTONIC SETTING OF FELSIC GNEISSES AND MAFIC ROCKS

The tectonic setting of the basin in which the Archean supracrustal rocks of the Blacktail Mountains were deposited must be compatible with the lithologic and geochemical characteristics of the protoliths of the felsic gneisses and mafic rocks. First, the lithologic characteristics of the protolith are reviewed in the following text. Lithologic characteristics serve to constrain the possible tectonic settings established by geochemical analyses. Next, trace-element characteristics (Rb vs. Y+Nb) of the felsic gneisses are analyzed to determine the tectonic environments in which these volcanic rocks may have been generated. Subsequently, major-element geochemistry of the felsic gneisses is evaluated to determine the tectonic environment in which the volcanic rocks were deposited. Then, Paleozoic basin analogues to this Archean basin are established by comparing geochemistry of the felsic gneisses to major element geochemistry of Paleozoic rocks of known tectonic setting. Lastly, since the type of basement can differentiate between basin types, available evidence for basin basement is reviewed.

The tectonic setting of the basin in which the supracrustal rocks were deposited must be compatible with the inferred protoliths of the felsic gneisses and mafic rocks. The protolith consists of a bimodal rhyolite/dacite-basalt suite. Acidic (69-76 wt.% SiO_2) dacits and

rhyolites are dominant and include minor volumes of intermediate (55-60 wt.% SiO_2) andesites. Volcanic and volcaniclastic deposits have been reworked and interlayered with carbonates. These deposits are also interlayered with primitive tholeiitic to slightly calc-alkalic basalt (Mg' = 0.38-0.59) sills and/or flows and rare basaltic komatiite (Mg' = 0.77) sills and/or flows.

An appropriate tectonic environment is required for the generation of the original volcanic suite. Pearce and others (1984) have applied trace element analyses to discriminate between tectonic regimes in which granites (senso lato, any plutonic rock containing greater than five modal percent quartz) are generated. Tectonic regimes for granite plutons should also apply to their extrusive equivalents. Data from the felsic gneiss samples of the Blacktail Mountains are plotted on a Rb-(Y+Nb) diagram (Pearce and others, 1984) in Figure 21. Four tectonic environments are represented on this diagram: volcanic arc granites (VAG), within plate granites (WPG), syn-collisional granites (SYN-COLG), and ocean-ridge plagiogranites (ORG). VAG includes tholeiitic and calc-alkalic oceanic arc granites, and active continental margin granites. WPG includes intracontinental ring-complex and graben granites, attenuated continental crust granites and ocean island granites. SYN-COLG includes syn-tectonic granites produced by continent-continent, continent-arc and arc-arc collisions. ORG includes ocean-ridge plagiogranites and granites of spreading ridges in back-arc basins. Felsic gneiss samples plot in a pattern which overlaps the VAG and WPG fields. The dominant rhyolite-to-dacite composition of these samples precludes an oceanic island arc

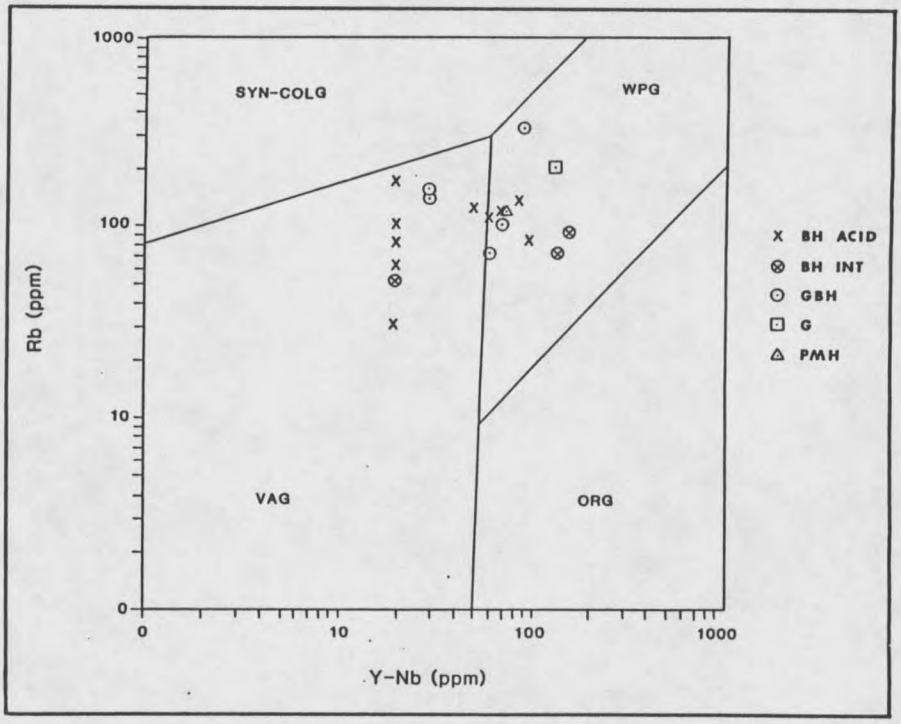

Figure 21. Rb values are plotted against Y+Nb values of the felsic gneisses to identify probable tectonic environments in which the volcanic protoliths were generated (Pearce and others, 1984). The fields represent volcanic arc granites (VAG), ocean-ridge plagiogranites (ORG), within plate granites (WPG), and syn-collisional granites (SYN-COLG).

environment for their generation. The most plausible environments are active continental margins of the VAG field; and intracratonic ring structures and grabens and attenuated continental crust of the WPG field. The overlapping pattern indicates either affinities with both granite types or contribution of volcanic rocks generated in both environments to the same basin.

McLennan (1984) reviewed methods that may be used to determine tectonic setting of basins. Of the major geochemical parameters, K_2O/Na_2O and FeO+MgO were found to be the most indicative of tectonic

environment. Fore-arc basin deposits tend to have low K_2O/Na_2O (less than 0.50) and high FeO+MgO (greater than 8 wt.%). Trailing edge deposits have the opposite characteristics; high K_2O/Na_2O (greater than 1.0) and low (FeO+MgO less than 5 wt.%). Back-arc and leading edge basin deposits show intermediate values. K_2O/Na_2O and FeO+MgO parameters for the felsic gneiss samples are presented in Table 3. Seven of thirteen BH samples and two of five GBH samples have intermediate K_2O/Na_2O and FeO+MgO values. Five of thirteen BH, three of five GBH, and the single G and PMH samples have values compatible with trailing edge deposits. Only one sample (BHM-1) has values compatible with a fore-arc basin. Most samples have either intermediate values, indicating a back-arc or leading edge basin, or high K_2O/Na_2O and low FeO+MgO values suggesting a trailing edge basin.

Bhatia (1983) used major element analyses of Paleozoic sandstones of known tectonic setting to identify fields characteristic of those tectonic environments on diagrams of Fe_2O_3+MgO plotted against TiO_2, Al_2O_3/SiO_2, K_2O/Na_2O and $Al_2O_3/(CaO+Na_2O)$. Data for the felsic gneisses of the Blacktail Mountains are plotted in Figures 22(a-d). Bhatia (1983) used four simplified plate tectonic classifications in his discrimination, summarized in Table 5 (described also in Bhatia and Cook, 1986).

Samples from the Blacktail Mountains plot in a somewhat scattered pattern across these diagrams. The scatter may reflect changes in the nature of volcanic activity and/or the composition of continental crust from Archean to Phanerozoic time. Alternatively, the scatter may be an effect of weathering and/or hydrothermal alteration of the original

Table 5. Tectonic environments used by Bhatia (1983) and used in Figure 22 and Figure 23 are summarized in this table.

OCEANIC ISLAND ARC: basins adjacent to oceanic island arcs (e.g., Marianas) and island arcs partly formed on thin continental crust (e.g., Aleutian Islands). Sediment is derived from undissected calc-alkalic or tholeiitic magmatic arcs and deposited in fore-arc and back-arc basins.

CONTINENTAL ISLAND ARC: back-arc basins on the continental side of island arcs which formed on well-developed continental crust (e.g., Japan Sea) or basins adjacent to arcs formed on thin continental margins (e.g., Cascades, western USA). Sediment is derived from dissected magmatic arcs and recycled orogens and then deposited in inter-arc, back-arc or fore-arc basins.

ACTIVE CONTINENTAL MARGIN: basins adjacent to Andean-type magmatic arcs on thick continental margins (e.g., North Chile, Peru) or adjacent to transverse plate boundaries (e.g., Pacific Ocean adjacent to California). Basins are developed on or adjacent to thick continental crust. Sediments are derived from granitic gneisses of uplifted basement, or siliceous volcanic rocks and deposited in marginal retro-arc and pull-apart basins.

PASSIVE MARGIN: basins are developed on rifted continental margins (e.g., Atlantic coast) remnant ocean basins adjacent to collisional orogens, and inactive or extinct convergent margins. Intracratonic and rift-bounded grabens are included. Sediments are derived from older continental crust and include compositionally mature varieties.

---

volcanic/volcaniclastic sequences. However, samples of BH-ACID, GBH, PMH and G (acidic felsic gneisses) plot in or near the active continental margin and passive margin fields of Figures 22(a) and 22(b). In Figure 22(c), data plot parallel to the alignment of the continental island arc, active continental margin, and passive margin fields. In Figure 22(d), most felsic gneiss data plot in the continental island arc, active continental margin and passive margin fields.

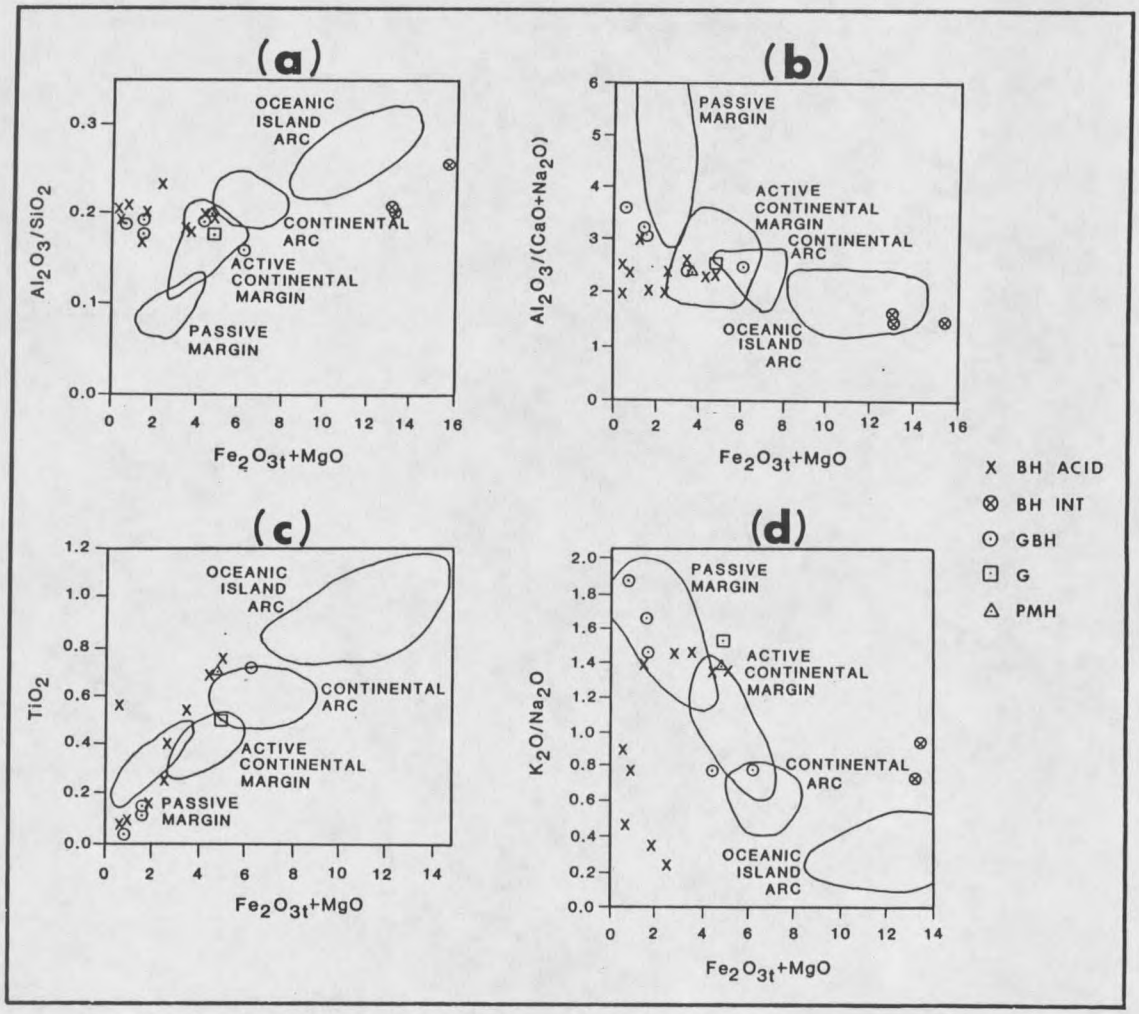

Figure 22. Fe_2O_3+MgO values are plotted against other major element parameters of the felsic gneisses to distinguish tectonic setting in which the protolith volcanic rocks were deposited. Fields are derived from Paleozoic rocks of known tectonic setting (Bhatia, 1983).

Geochemical analyses of the felsic gneisses require that the protolith consist of volcanic rocks and volcaniclastic rocks. Passive margin environments accommodate sequences which include compositionally

mature sediments and may be ruled out as a possible environment for the felsic gneisses. The most likely environment appears to be associated with Bhatia's (1983) ACTIVE CONTINENTAL MARGIN field.

Bhatia (1983) used the same major-element chemistry of sandstones of known tectonic environments as in Figure 22 to generate a discriminant function analysis, presented here in Figure 23, which accounts for variations in eleven major elements. A plot of two discriminant functions, DF1 vs. DF2, provides excellent separation of known sandstones into the same four tectonic environment fields shown in Figure 22. The two discriminant functions are of the following form (coefficients are multiplied by wt.% oxide):

$$DF1 = -0.0447(SiO_2) - 0.972(TiO_2) + 0.008(Al_2O_3) - 0.267(Fe_2O_3) + 0.208(FeO) - 3.082(MnO) + 0.140(MgO) + 0.195(CaO) + 0.719(Na_2O) - 0.032(K_2O) + 7.510(P_2O_5) + 0.303.$$

$$DF2 = -0.421(SiO_2) + 1.988(TiO_2) - 0.526(Al_2O_3) - 0.551(Fe_2O_3) - 1.610(FeO) + 2.720(MnO) + 0.881(MgO) - 0.907(CaO) - 0.177(Na_2O) - 1.840(K_2O) + 7.244(P_2O_5) + 43.57.$$

DF1 has a high loading of CaO and Na_2O and is mainly influenced by plagioclase and volcanic fragments in sandstone. DF1 separates highly feldspathic suites from less feldspathic suites. DF2 has a high loading of SiO_2 and CaO and discriminates suites having high-quartz contents from those with less quartz. Data are plotted on a DF1 vs. DF2 diagram (Bhatia, 1983) in Figure 23. Nearly all acidic felsic gneiss samples plot in the active continental margin field. The BH-INT samples plot in the oceanic island arc field.

Condie and DeMalas (1985) and Condie (1986) modified the fields on the major element discrimination diagrams of Bhatia (1983) in their study of Proterozoic supracrustal rocks of the southwestern U.S., including the Pinal Schist. The modified fields occupy the same space on the diagrams, but have been renamed to accommodate additional environments (see Table 6). The fields affected by Condie and DeMalas

Table 6. Tectonic environments used by Bhatia (1983) (cf. Table 5) have been modified by Condie and DeMalas (1985) and Condie (1986).

Bhatia (1983)	Condie and DeMalas (1985) and Condie (1986)
OCEANIC ISLAND ARC	OCEANIC ARC
CONTINENTAL ISLAND ARC	CONTINENTAL ARC
ACTIVE CONTINENTAL MARGIN	COLLISIONAL OROGEN, CONTINENTAL RIFT AND BACK-ARC BASIN ON CONTINENTAL CRUST
PASSIVE MARGIN	CRATONIC BASIN

(1985) and Condie (1986) are primarily ACTIVE CONTINENTAL MARGIN and to a lesser extent PASSIVE MARGIN. Under re-assignment, the ACTIVE CONTINENTAL MARGIN field includes deposition in a) retro-arc (on the continental side) and marginal basins (on the oceanic side) adjacent to an Andean-type arc, b) pull-apart basins adjacent to transverse continental margins, c) continental rifts, and d) Japan Sea-type, back-arc basins. The continental rift environment, in Bhatia's (1983) PASSIVE MARGIN field, is re-assigned to the ACTIVE CONTINENTAL MARGIN

field, apparently in recognition of volcanic and volcaniclastic rocks that may be present in continental rift settings which were not originally considered by Bhatia (1983).

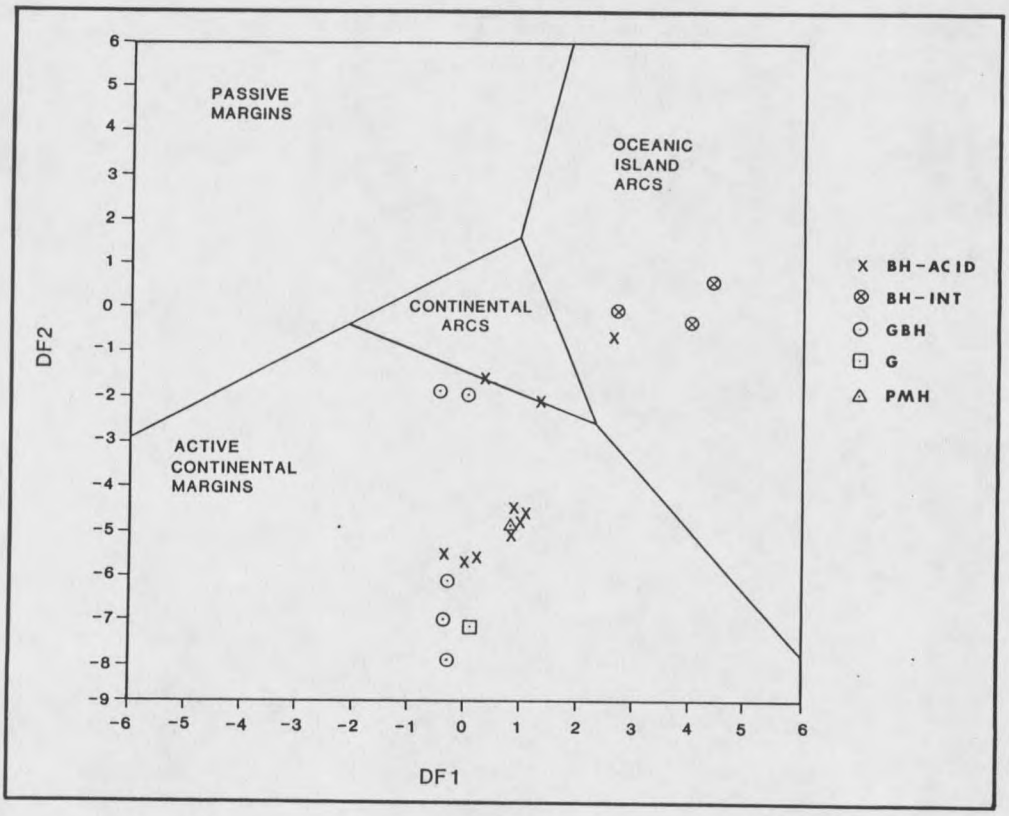

Figure 23. Multivariable discriminant function analyses, DF1 vs. DF2, distinguish tectonic settings of the felsic gneisses. Fields are derived from analyses of Paleozoic rocks of known tectonic setting (Bhatia, 1983).

Tectonic setting must also be compatible with available evidence for basin basement. Basement rocks may consist of continental crust, attenuated continental crust which is transitional between continental crust and oceanic crust, or oceanic crust. Remnants of oceanic crust have not been recognized in the Archean rocks exposed in the northwestern Wyoming Province. Possible remnants of oceanic crust are

the small ultramafites that are described in the Blacktail Mountains and the ultramafites that have been studied in detail in the Ruby Range, north of the Blacktail Mountains (Desmarais, 1981). However, none of these ultramafites have been confidently ascribed to tectonically emplaced ocean crust. Even if the ultramafites are oceanic crust remnants, they are not present in volumes sufficient to suggest an extensive basement comprised of oceanic crust. However, remnants of a basement comprised of continental crust may be present as slices of older quartzofeldspathic gneisses that have been tectonically interlayered with supracrustal sequences which are also now quartzofeldspathic gneisses. Although such tectonic slices have yet to be recognized, additional geochemical studies and detailed age dating may separate the supracrustal rocks from the continental crust basement. Due to the paucity of recognized remnants of oceanic crust, the basement for this basin is inferred to consist of continental crust or transitional continental crust.

Geochemical discrimination allows selection of a range of tectonic environments that are compatible with characteristics of the felsic gneisses. Magmas which produced the acidic felsic volcanics may have been generated in a variety of environments, including active continental margins, intracontinental ring complexes and grabens, and attenuated continental crust. The most probable tectonic environments of deposition include the following: basins associated with collisional or transverse plate boundaries; such as retro-arc and marginal basins adjacent to an Andean-type arc, and pull-apart basins; and basins associated with extensional plate boundaries; such as

continental rifts and Japan Sea-type, back-arc basins. The basements of these potential basins are inferred to consist of continental or transitional continental crust. The felsic gneisses are also interlayered with small quantities of tholeiitic to slightly calc-alkalic basalts and rare basaltic komatiites. An extensional or transverse plate boundary is more compatible with the presence of these mantle derived, mafic rocks than a collisional environment. However, continental rifting may also occur in a retro-arc setting. The probable tectonic environments for generation and deposition of the felsic gneisses and mafic rocks are pull-apart basins, continental rifts (perhaps developed in a retro-arc setting) and Japan Sea-type, back-arc basins.

The probable environments can be narrowed to one preferred environment if the composition and relative volumes of volcanic protolith are considered. Pull-apart basins are unlikely because modern basins of this type are associated with deposition of clastic sediments eroded from adjacent land masses, and not volcanic sedimentation. The Japan Sea-type, back-arc basin is unlikely because modern basins of this nature are host to andesite-dominated felsic volcanism and the sequence in the Blacktail Mountains is dominated by rhyolites and dacites. Modern continental rift settings are associated with bimodal rhyolite-basalt volcanism, and in at least some cases rhyolite is predominant. The preferred setting for deposition of the supracrustal sequence in the Blacktail Mountains is in a continental rift that may have developed in a retro-arc environment.

Other terranes have been described that have lithologic and chemical characteristics similar to the Archean supracrustal sequence in the Blacktail Mountains and have been assigned similar tectonic settings. For example, the Archean Nsuze Group of the Pongola Sequence in South Africa is a volcano-sedimentary succession deposited on continental crust (Armstrong and others, 1986). Primary textural features that survived greenschist metamorphism and gentle deformation suggest that the volcanics were deposited upon a granitoid paleosaprolite. The Nsuze volcanics have tholeiitic characteristics and include basalts, andesites and rhyolites. However, lavas of intermediate composition (i.e. andesites) are dominant. These volcanic rocks are characterized by complex intercalation of basaltic to rhyolitic flows that were probably extruded simultaneously. Volcanism was succeeded by alluvial sedimentation deposited within a macrotidal marine basin under stable intracratonic conditions. The Nsuze Group and the volcanic sequence in the Blacktail Mountains are similar in depositional setting, range of composition, intercalation of different compositions, and association with sediments. However, the sequence in the Blacktail Mountains does have basalts with higher Mg' and a greater proportion of acidic to intermediate volcanic rocks than the Nsuze Group.

The Pinal Schist, described by Copeland and Condie (1986), provides an early Proterozoic analogue to the sequence in the Blacktail Mountains. The Pinal Schist of southeastern Arizona consists of eastern and western assemblages. The western assemblage is composed largely of quartz-wacke turbidites. The eastern assemblage is composed

largely of bimodal volcanics with variable amounts of sediment. The mafic rocks are a minor component in the western assemblage and are a major constituent in the eastern assemblage. Mafic rocks are typically olivine-normative tholeiites with Mg' = 40-60. Several mafic rocks have Mg' greater than 70 and are similar to basaltic komatiites. The felsic rocks occur in the western assemblage predominantly as hypabyssal intrusions and in the eastern assemblage as tuffs, breccias and lesser volumes of hypabyssal intrusives. The felsic volcanics and volcaniclastic sediments are rhyolitic to rhyodacitic in composition. The depositional environment of the western assemblage is thought to have been an intra-arc basin or an aulacogen. The eastern assemblage is inferred to be a remnant of a major continental magmatic arc system. The nature of the boundary between these assemblages is not well understood. The Archean sequence in the Blacktail Mountains has similarities to both assemblages and may represent an environment intermediate between that of the eastern and western assemblages of the Proterozoic Pinal Schist.

CHAPTER 9

PRECAMBRIAN EVOLUTION OF THE SUPRACRUSTAL SEQUENCE

Available evidence allows the reconstruction of Precambrian events through which the supracrustal rocks of the Blacktail Mountains has evolved. The sequence includes events beginning with deposition of the supracrustal sequence, continuing through deformation and high-grade metamorphism, and terminating with emplacement of the gabbroic dikes. These events are described in the following text.

Rhyolitic to dacitic volcanics were erupted on continental crust and deposited into a continental rift basin, possibly on the continental side of an Andean-type arc. Intermediate andesitic volcanics were intercalated with the acidic volcanics. The andesites may have been generated in the continental rift or contributed from an adjacent Andean-type arc. The basin evolved sufficiently to accommodate a body of water and the deposition of carbonate layers. Tholeiitic to slightly calc-alkalic basalts and rare basaltic komatiites were interlayered with the felsic volcanics as flows and/or sills. The basalts and basaltic komatiites were derived from a mantle source.

The basin collapsed and its contents were subjected to granulite-grade metamorphism, at temperatures of 740-810^{o}C and minimum pressures of 5.1-6.2 kilobars. Basin sediments must have been buried to at least 20 kilometers in order to achieve granulite-grade metamorphism

(Windley, 1984). The most probable way that a rock sequence may be buried 20 kilometers is by having one section of crust thrust over another. Since the basin is developed entirely within continental crust, the only crustal sections available to be thrust one over another are continental. Therefore, the preferred mechanism for collapse of the basin involves the convergence of the continental masses that bounded the continental rift basin and burial of the basin strata to at least 20 kilometers beneath a section of continental crust. Collapse of the basin and attendant high-grade metamorphism occurred about 3.08 Ga ago (from Giletti, 1966).

The peak metamorphic event was accompanied by local *in situ* anatexis and formation of stromatic migmatites. During this event, basin strata were subjected to at least one and possibly two isoclinal folding events (F1 and F2), which transposed original compositional layering. Isoclinal folds were refolded into open folds (F3). Open folding is interpreted to be an effect of progressive deformation succeeding isoclinal folding.

Lower temperatures are recorded by garnet rims and biotite grains tangential to garnet grains (500-550^{o}C). Lower temperature equilibration also resulted in the development of myrmekites and albite rims. Penetrative deformation was apparently not associated with this re-equilibration. Lower equilibration temperatures may be an effect of a regional, retrograde, thermal event or elevation of the block to higher crustal levels and coeval cooling of the sequence after peak metamorphism.

Finally, Proterozoic gabbroic dikes were emplaced along west to northwest trends. Emplacement of these dikes may have been the result of extensional tectonics related to opening of the Belt Basin (Schmidt and Garihan, 1986).

CHAPTER 10

CONCLUSIONS

The goal of this study was to contribute to the understanding of high-grade quartzofeldspathic gneiss terranes in two ways. The first contribution was to determine methods that are most useful in differentiating between supracrustal and plutonic protoliths, and which do not rely on primary sedimentary or igneous textures. The second contribution was to determine methods useful in distinguishing the tectonic setting in which an Archean supracrustal sequence may be deposited. Methods of protolith discrimination and tectonic setting discrimination were applied to a sequence of high-grade QFGs with disputed protolith. That case study is reviewed below.

A sequence of QFG within the Blacktail Mountains, referred to by previous workers as "Dillon Granite Gneiss" (e.g., Scholten and others, 1955), is also mapped in the Ruby Range to the north. The protolith of the "Dillon Granite Gneiss," in its original type locality in the Blacktail Mountains, is supracrustal (Clark and Mogk, 1985, 1986; and this study). Research in the Ruby Range has not uniquely determined whether the "Dillon Granite Gneiss" is of plutonic or supracrustal origin (e.g., Garihan and Williams, 1976; Garihan, 1979). Research on similar pink granites in Sri Lanka provides an analogue to this enigma. Munasinghe and Dissanayake (1980) inferred that the pink granite bodies that were interlayered with metapelites

were anatectic melts. Descriptions of the granitic layers by Munasinghe and Dissanayake (1980) and Perera (1983) are similar to descriptions of some horizons of felsic gneisses in the Blacktail Mountains and to descriptions of the "Dillon Granite Gneiss" in the Ruby Range (Garihan, 1979; Karasevich and others, 1981; and Schaefer, 1986). The granitic bodies in Sri Lanka form conformable layers and have sharp boundaries with interlayered metasediments. The granitic layers and interlayered metasediments have been isoclinally folded. The granitic layers are nearly massive, medium grained and have abundant coarse-grained laminae. Modal mineralogy of the Sri Lanka granitic layers plots in the granite field on the igneous rock classification diagram of Streckheisen (1976). However, Perera (1983) has subsequently documented an origin by treptometamorphism for these pink granites. Dietrich (1963) used the term "treptometamorphism" to describe the formation of granites by isochemical metamorphism of sedimentary rocks. Other research has documented the supracrustal nature of rocks of "granitic" appearance. For example, Dietrich (1960) describes outcrops of recrystallized arkoses in Norway that have granitic appearances. Also, Engel and Engel (1958) describe the progressive granitization associated with increasing metamorphic grade of graywackes in Maine. Quartzofeldspathic gneisses in the Ruby Range, correlated with QFGs in the Blacktail Mountains, that have "distinctive" plutonic, granite-like appearances could have had supracrustal parent rocks that have been isochemically metamorphosed.

This study has shown that a continental rift basin, possibly developed in a retro-arc setting, is a viable tectonic setting for

generation and deposition of at least one Archean supracrustal sequence in the northwestern Wyoming Province. This environment is also capable of accommodating marble, quartzite, iron formation and metapelite-bearing sequences, similar to those of the Ruby Range, if the rift basin were to widen and stabilize. Tectonic settings (but not necessarily the same basin) presented here for the supracrustal sequence of the Blacktail Mountains may be applicable to other supracrustal sequences with similar characteristics elsewhere in the northwestern Wyoming Province.

REFERENCES CITED

Armstrong, N.V., Wilson, A.H., and Hunter D.R., 1986, The Nsuze Group, Pongola Sequence, South Africa: geochemical evidence for Archaean volcanism in a continental setting: Precambrian Research, v. 34, p. 175-203.

Barley, M.E., 1986, Incompatible-element enrichment in Archean basalts: a consequence of contamination by older sialic crust rather than mantle heterogeneity: Geology, v. 14, no. 11, p. 947-950.

Basaltic Volcanism Study Project, 1981, Basaltic volcanism on the terrestrial planets: New York, Pergamon Press, 1286 p.

Beach, A., and Tarney, J., 1978, Major and trace element patterns established during retrogressive metamorphism of granulite-facies gneisses, NW Scotland: Precambrian Research, v. 7., p. 325-348.

Berg, R.B., 1979, Precambrian geology of the west part of the Greenhorn Range, Madison County, Montana: Montana Bureau of Mines and Geology Geologic Map 6.

Bergantino, R.N., and Clark, M.L., 1985, Structure contour map on the top of Precambrian crystalline rocks, Montana: Montana Bureau of Mines and Geology Open File Report MBMG-158.

Bhatia, M.R., 1983, Plate tectonics and geochemical composition of sandstones: Journal of Geology, v. 91, no. 6, p. 611-627.

Bhatia, M.R., and Crook A.W., 1986, Trace element characteristics of graywackes and tectonic setting discrimination of sedimentary basins: Contributions to Mineralogy and Petrology, v. 92, p. 181-193.

Brownlow, A.N., 1979, Geochemistry: Englewood Cliffs, New Jersey, Prentice-Hall Inc., 498 p.

Carmichael, I.S.E., Turner, F.S., and Verhoogen, J., 1974, Igneous Petrology: New York, McGraw-Hill Book Company, 739 p.

Casella, S.J., Levay, J., Eble, E., Hirst, G., Huffman, K., Lahti, V., and Metzger, R., 1982, Precambrian geology of the southwest Beartooth Mountains, Yellowstone National Park, Montana and Wyoming, in Mueller, P.A., and Wooden, J.L., eds., Precambrian geology of the Beartooth Mountains, Montana and Wyoming: Montana Bureau of Mines and Geology Special Publication 84, p. 1-24.

Clark, M.L., and Mogk, D.W., 1985, Development and significance of the Blacktail Mountains Archean Metamorphic Complex: Geological Society of America Abstracts with Program, v. 17, no. 4, p. 212.

_____. 1986, Tectonic setting of the Blacktail Mountains Archean supracrustal sequence, SW Montana: Geological Society of America Abstracts with Program, v. 18, no. 4, p. 346-347.

Condie, K.C., 1976, The Wyoming Archean Province in the western United States, in Windley, B.F., ed., The Early History of the Earth: New York, John Wiley and Sons, p. 499-510.

Condie, K.C., 1983, Plate Tectonics and Crustal Evolution: New York, Pergamon Press, 310 p.

Condie, K.C., 1986, Geochemistry and tectonic setting of early Proterozoic supracrustal rocks in the southwestern United States: Journal of Geology, v. 94, p. 845-864.

Condie, K.C., and DeMalas, J.P., 1985, The Pinal Schist; an early Proterozoic quartz-wacke association in southeastern Arizona: Precambrian Research v. 27, p. 337-356.

Copeland, P., and Condie, K.C., 1986, Geochemistry and tectonic setting of lower Proterozoic supracrustal rocks of the Pinal Schist, southeastern Arizona: Geological Society of America Bulletin, v. 97, p. 1512-1520.

Cullers, R.L., and Graf, J.L., 1984, Rare earth elements in igneous rocks of the continental crust; intermediate and sialic rocks - ore petrogenesis, in Henderson, P., ed., Rare earth element geochemistry: New York, Elsevier, p. 275-316.

Dahl, P.S., 1979a, Comparative geothermometry based on major-element and oxygen-isotope distributions in Precambrian metamorphic rocks from southwestern Montana: American Mineralogist, v. 64, p. 1280-1293.

_____. 1979b, Coexisting garnet and cordierite as indicators of retrograde metamorphic conditions in the Ruby Range, southwestern Montana: Contributions to Geology, v. 18, no. 2, p. 77-82.

Desmarais, N.R., 1981, Metamorphosed Precambrian ultramafic rocks in the Ruby Range, Montana: Precambrian Research, v. 16, p. 67-101.

Dietrich, R.V., 1960, Banded gneisses: Journal of Petrology, v. 1, p. 99-120.

Dietrich, R.V., 1963, Banded gneisses of eight localities: Norsk Geologisk Tidsskrift, v. 43, p. 89-119.

Duncan, M.S., 1976, Structural analysis of the pre-Beltian metamorphic rocks of the southern Highland Mountains, Madison and Silver Bow counties, Montana (Ph.D. thesis): Bloomington, Indiana, Indiana University, 222 p.

Dymek, R.F., 1983, Titanium, aluminum and interlayer cation substitutions in biotite from high-grade gneisses, west Greenland: American Mineralogist, v. 68, p. 880-899.

Ellis D.J., and Green, D.H., 1979, An experimental study of the effect of Ca upon garnet-clinopyroxene Fe-Mg exchange equilibria: Contributions to Mineralogy and Petrology, v. 71, p. 13-22.

Engel, A.E.J., and Engel, C.G., 1958, Progressive metamorphism and granitization of the major paragneiss, northwest Adirondack Mountains, New York, part I: Geological Society of America Bulletin, v. 69, p. 1369-1413.

Erslev, E.A., 1983, Pre-Beltian geology of the southern Madison Range, southwestern Montana: Montana Bureau of Mines and Geology Memoir 55, 26p.

Ganguly, J., and Saxena, S.K., 1984, Mixing properties of aluminosilicate garnets: constraints from natural and experimental data, and applications to geothermo-barometry: American Mineralogist, v. 69, p. 88-97.

Ganuly, J., and Saxena, S.K., 1985, Mixing properties of aluminosilicate garnets: constraints from natural and experimental data, and applications to geothermo-barometry: clarifications: American Mineralogist, v. 70, p. 1320.

Garihan, J.M., 1979, Geology and structure of the central Ruby Range, Madison County, Montana: Geological Society of America Bulletin, part II, v. 90, p. 695-788.

Garihan, J.M., and Okuma, A.F., 1974, Field evidence suggesting a non-igneous origin for the Dillon quartzofeldspathic gneiss, Ruby Range, southwestern Montana (abs): Geological Society of America Abstracts with Programs, v. 6, no. 6, p. 510.

Garihan, J.M., and Williams, K., 1976, Petrography, modal analyses and origin of Dillon quartzofeldspathic and pre-Cherry Creek gneisses, Ruby Range, southwestern Montana: Northwest Geology, v. 5, p. 42-49.

Giletti, B., 1966, Isotopic ages from southwestern Montana: Journal of Geophysical Research, v. 71, p. 4029-4036.

Giletti, B., 1971, Discordant isotopic ages and excess argon in biotites: Earth and Planetary Science Letters, v. 110, p. 157-164.

Green, D.H., 1975, Genesis of Archean peridotitic magmas and constraints on Archean geothermal gradients and tectonics: Geology, v. 3, p. 15-18.

Green, D.H., 1981, Petrogenesis of Archean ultramafic magmas and implications for Archean tectonics, in Kroner, A., ed., Precambrian plate tectonics: New York, Elsevier Scientific Publishing Company, p. 469-489.

Guidotti, L.V., Cheney, J.T., and Guggenheim, S., 1977, Distribution of titanium between coexisting muscovite and biotite in pelitic schists from northwestern Maine: American Mineralogist, v. 62, p. 438-448.

Hadley, J.B., 1969a, Geologic map of the Cameron Quadrangle, Madison County, Montana: U.S. Geological Survey Quadrangle Map GQ-813.

_____. 1969b, Geologic map of the Varney Quadrangle, Madison County, Montana: U.S. Geological Survey Geologic Quadrangle Map GQ-814.

_____. 1980, Geology of the Varney and Cameron quadrangles, Madison County, Montana: U.S. Geological Survey Bulletin 1459, 108 p.

Hanson, G.N., 1980, Rare earth elements in petrogenetic studies of igneous systems: Annual Review of Earth and Planetary Science, v. 8, p. 371-406.

Heinrich, E.W., 1948, Pre-Beltian rocks near Dillon, Montana (abs): Geological Society of America Bulletin, v. 59, no. 12, pt. 2, p. 1329.

Heinrich, E.W., 1950, Sillimanite deposits of the Dillon region, Montana: Montana Bureau of Mines and Geology, Memoir 30, p. 6-8.

Heinrich, E.W., 1953, Pre-Beltian geologic history of Montana (abs): Geological Society of America Bulletin, v. 64, no. 12, p. 1432.

Heinrich, E.W., and Rabbit, J.E., 1960, Pre-Beltian geology of the Cherry Creek and Ruby Mountains areas, southwestern Montana: Montana Bureau of Mines and Geology, Memoir 38, 40 p.

Hobbs, B.E., Means, W.D., and Williams, P.F., 1976, An outline of structural geology: New York, John Wiley and Sons, Inc., 571 p.

Immega, I.P., and Klein, C., Jr., 1976, Mineralogy and petrology of some metamorphic Precambrian iron formations in southwestern Montana: American Mineralogist, v. 61, p. 1107-1144.

Indares, A., and Martignole, J., 1985, Biotite-garnet geothermometry in the granulite facies; the influence of Ti and Al in biotite: American Mineralogist, v. 70, p. 272-278.

Irvine, T.N., and Baragar, W.R.A., 1971, A guide to the chemical classification of the common volcanic rocks: Canadian Journal of Earth Sciences, v. 8, p. 523-548.

James, H.L., and Hedge, C.E., 1980, Age of the basement rocks of southwest Montana: Geological Society of America Bulletin, v. 9, pt. 1, p. 11-15.

Johannes, W., and Gupta, L.N., 1982, Origin and evolution of a migmatite: Contributions to Mineralogy and Petrology, v. 79, p. 114-123.

Karasevich, L.P., 1980, Structure of the pre-Beltian metamorphic rocks of the northern Ruby Range, southwestern Montana (M.S. thesis): State College, Pennsylvania, Pennsylvania State University, 172 p.

Karasevich, L.P., 1981, Geologic map of the northern Ruby Range, Madison County, Montana: Montana Bureau of Mines and Geology Geologic Map 25.

Karasevich, L.P., Garihan, J.M., Dahl, P.S., and Okuma, A.F., 1981, Summary of Precambrian metamorphic and structural history, Ruby Range, southwest Montana: Montana Geological Society Annual Field Conference Guidebook, p. 225-237.

Karlstrom, K.E., 1979, Early Proterozoic geology of the Wyoming Province: Contributions to Geology, v. 17, no. 2, outside covers and inside rear cover.

Kleinschmidt, J.C., 1981, Bedrock petrology of the Horse Creek and Wall Creek drainages, Gravelly Range, Madison County, Montana (M.S. thesis): Butte, Montana, Montana College of Mineral Science and Technology, 72 p.

Kwak, T.H.P., 1968, Titanium in biotite and muscovite as an indication of increasing metamorphic grade in almandine amphibolite facies rocks from Sudbury, Ontario: Geochimica et Cosmochimica Acta, v. 32, p. 1222-1229.

Leake, B.E., and Singh, D., 1986, The Delaney Dome Formation, Connemara, West Ireland, and the geochemical distinction of ortho- and para-quartzofeldspathic rocks: Mineralogical Magazine, v. 50, p. 205-215

Leyreloup, A., Dupuy, C., and Andriambololona, R., 1977, Catazonal xenoliths in French Neogene volcanic rocks: constitution of the lower crust: Contributions to Mineralogy and Petrology, v. 62, p. 283-300.

MacGeehan, P.J., and MacLean, W.H., 1980, An Archean sub-seafloor geothermal system, 'calc-alkaline' trends and massive sulfide genesis: Nature, v. 286, p. 767-771.

McKenzie, D., and Weiss, N., 1975, Speculations on the thermal and tectonic history of the earth: Geophysical Journal of the Royal Astronomical Society, v. 42, p. 131-174.

McLennan, S.M., 1984, Petrological characteristics of Archean graywackes: Journal of Sedimentary Petrology, v. 54, no. 3, p. 889-898.

McThenia, A.W., Jr., 1960, Geology of the Madison River canyon area north of Ennis, Montana: Billings Geological Society 11th Annual Field Conference Guidebook, p. 155-164.

Millholland, M.A., 1976, Mineralogy and petrology of Precambrian metamorphic rocks of the Gravelly Range, southwestern Montana (M.A. thesis): Bloomington, Indiana, Indiana University, 134 p.

Mogk, D.W., 1984, Petrology, geochemistry and structure of an Archean terrane in the North Snowy Block, Beartooth Mountains, Montana (Ph.D. thesis): Seattle, Washington, University of Washington, 440 p.

Mogk, D.W., and Henry, D.J., 1987, Metamorphic petrology of the northern Archean Wyoming Province, SW Montana; evidence for Archean collisional tectonics: VII Ruby Colloquium on metamorphic terranes, in press.

Mueller, P.A., and Cordua, W.S., 1976, Rb-Sr whole rock ages of gneisses from the Horse Creek area, Tobacco Root Mountains, Montana: Isochron West, no. 16, p. 33-36.

Mueller, P.A., and Wooden, J.L., eds., 1982, Precambrian geology of the Beartooth Mountains, Montana and Wyoming: Montana Bureau of Mines and Geology Special Publication 84, 167 p.

Mueller, P.A., Wooden, J.L., Schluz, K., and Bowes, D.R., 1983, Incompatible-element-rich andesitic amphibolites from the Archean of Montana and Wyoming: evidence for mantle metasomatism: Geology, v. 11, p. 203-206.

Mueller, P.A., Wooden, J.A., Henry, D.J., and Bowes, D.R., 1985, Archean crustal development of the eastern Beartooth Mountains, Montana and Wyoming, in Czmanske, G.K., and Zientek, M.L., eds., The Stillwater Complex, Montana; geology and guide: Montana Bureau of Mines and Geology Special Publication 92, p. 9-20.

Munasinghe, T., and Dissanayake, C.B., 1980, Pink granites in the Highland Series of Sri Lanka--a case study: Journal of the Geological Society of India, v. 21, p. 446-452.

Newton, R.C., 1983, Geobarometry of high-grade metamorphic rocks: American Journal of Science, v. 183-A, p. 1-28.